Elsevier Editorial System(tm) for Geomorphology
Manuscript Draft

Manuscript Number: GEOMOR-4648

Title: Landslide Inventories for Climate Impacts Research in the European Alps

Article Type: Research Paper

Keywords: Landslides, Hazards, Climate Change, Scaling, Power-Law

Corresponding Author: Dr Liam Reinhardt, Ph.D.

Corresponding Author's Institution: University of exeter

First Author: Joanne Laura Wood, MSc

Order of Authors: Joanne Laura Wood, MSc; Stephan Harrison; Liam Reinhardt

Abstract: Landslides present a geomorphological hazard in Alpine regions, threatening life, infrastructure and property. Here we present the development of a new regional landslide inventory (RI) for the European Alps. This database provides a substantial temporal and spatial picture of landsliding in the Alps; with particular focus on the Swiss and French Alps. We use segmented models to evaluate recording bias in the temporal record. Scaling relationships are used to calculate landslide area based on a given volume for similar types of landslide; 9.5% (n=752 of a total of 7919) of landslides in the RI have area data recorded; this figure is based on both the source data and areas calculated from the scaling relationship. Using a power-law we demonstrate that the log-linear trend, which exists between landslide area and frequency in inventories, is present for this historical dataset, however, none of the individual databases, nor a unification of these, contains a complete record. We conclude by discussing applications of this dataset for the detection and attribution of climate change to the frequency and magnitude of landslides in this region however, stress the implications for this based on the completeness of such datasets.

Suggested Reviewers: Oliver Korup
korup@geo.uni-potsdam.de
His knowledge and expertise with landslide inventories.

Bruce Malamud
bruce.malamud@kcl.ac.uk
His expertise with the application of the power-law distribution as described and used in this paper.

Miet Van Den Eekhaut
miet.van-den-eeckhaut@jrc.ec.europa.eu
For her knowledge of landslide databases in Europe, and for her perspectives on hazard and risk

Cover Letter

Peter Lanyon Building
Penryn Campus
Treliever Road
Penryn
Cornwall
TR10 9FE
U.K.

5 February 2014

Dear Editors,

Please find attached our article "*Landslide Inventories for Climate Impacts Research in the European Alps*" for consideration for publication in Geomorphology.

The manuscript describes and analyses a new landslide inventory, spanning six centuries and covering both the French and Swiss Alps. This inventory is, to our knowledge, unique in its temporal and geographical coverage, and in its detail, including information on geology, topography and size; which have been extracted and sampled into the inventory through methods detailed in this manuscript. The compilation of the inventory from several previously existing datasets is described, and methods for filling in missing data (such as area and volume data through the use of scaling relationships) are documented. We discuss the temporal resolution of the dataset through the use of segmented models, and then investigate the frequency-area distribution based on this, and in the context of other studies.

This paper should attract a wide readership from researchers interested in risk and hazard mapping, those interested in further developing and analysing this unique dataset, and from those using our methods as a template for the maintenance and collation of landslide inventories in other regions.

We appreciate your consideration of this manuscript for publication.

Yours sincerely

Joanne Wood
University of Exeter
Corresponding author email address: Liam.Reinhardt@Exeter.ac.uk

Landslide Inventories for Climate Impacts Research in the European Alps

Wood, J.L., Harrison, S. and Reinhardt, L.

Corresponding author: Liam Reinhardt Email: Liam.Reinhardt@Exeter.ac.uk
University of Exeter, College of Life and Environmental Sciences
Peter Lanyon Building
Penryn Campus
Treliever Road
Penryn
Cornwall
TR10 9FE
Tel: +44 (0)1326 371868

Abstract

Landslides present a geomorphological hazard in Alpine regions, threatening life, infrastructure and property. Here we present the development of a new regional landslide inventory (RI) for the European Alps. This database provides a substantial temporal and spatial picture of landsliding in the Alps; with particular focus on the Swiss and French Alps. We use segmented models to evaluate recording bias in the temporal record. Scaling relationships are used to calculate landslide area based on a given volume for similar types of landslide; 9.5% (n=752 of a total of 7919) of landslides in the RI have area data recorded; this figure is based on both the source data and areas calculated from the scaling relationship. Using a power-law we demonstrate that the log-linear trend, which exists between landslide area and frequency in inventories, is present for this *historical* dataset, however, none of the individual databases, nor a unification of these, contains a complete record. We conclude by discussing applications of this dataset for the detection and attribution of climate change to the frequency and magnitude of landslides in this region however, stress the implications for this based on the completeness of such datasets.

Key words: **Landslides, Hazards, Climate Change, Scaling, Power-Law**

Highlights:

- We present a newly collated landslide inventory for the European Alps
- We study the volume-area and frequency-magnitude statistics of landslides recorded
- We examine the recording of landslides through time to identify gaps and breaks
- The inventory follows a robust power-law distribution
- We discuss applicability to climate change studies and hazard assessment

[1]

Abbreviations

BRGM	French National Database of the Bureau de Recherches Géologiques et Minières
EPSG	European Petroleum Survey Group
GB	Geologische Bundesanstalt
LSS	Combination of "Slides" and *RTL*
QGIS	Quantum Geographic Information System
RI	Regional Inventory
RTL	Rotational/Translational Landslide
RTM	Service de Restauration des terrains en Montagne de l'Isere, Grenoble, France
WSL	Swiss Flood and Landslide Damage Database of the Swiss Federal Institute for Forest, Snow and Landscape Research

1 Introduction

In the European Alps mean annual air temperatures have risen ~2°C during the 20th Century and since the end of the Little Ice Age (Hæberli and Beniston, 1998) leading to widespread deglaciation and an increase in the frequency and magnitude of certain natural hazards such as glacial lake outburst floods, flooding, avalanches and landsliding (Katz and Brown, 1992; Keiler *et al*., 2010). While deglaciation in this area can be directly linked with this increase in temperature (Hæberli, *et al*., 1999; Reichert *et al*., 2002), recording of the intensity and frequency of mass movements in the region has been inconsistent over time, inhibiting our ability to test their relationship to changes in the climate. However, rising regional population and the growth of infrastructure in the Alps over past decades has necessitated a better understanding of the relationship between climate change and landsliding to enable planners and insurance groups to mitigate and manage landslide risks.

In the European Alps, landslides constitute a natural hazard. Understanding their distribution is important to the insurance industry and planners due to the damage they cause to infrastructure, property and life (e.g. Hilker *et* al., 2009; Mallet *et al*., 2010). This provides one of the key drivers for our research and there is considerable interest from the insurance industry in understanding how landslide risk may change in the European Alps. While most research tends to centre on basin scale landsliding, focussing on modelling and understanding the mechanisms and precursors that lead to landslide initiation, for planners, interests lay with the potential hazards associated with landslides and for the insurance industry, with the financial implications from damage caused by landsliding (Jaboyedoff *et al.*, 2003). This highlights the need for regional-scale approaches to understanding landslide risk.

Understanding landslide risk and hazard is a complex issue for heavily populated regions such as the Alps. For example, population density varies seasonally (Guzzetti, 2005) and property values fluctuate, changing the values of assets (Lee and Jones, 2004). In addition to this, varying landslide magnitude, velocity and the type of movement (hence trigger) will also have implications for potential losses (Lee and Jones, 2004) therefore, establishing patterns between the spatial and temporal distribution of landslides and their triggers can facilitate modelling future risk (e.g. Crozier and Glade, 2004; Van Beek and Van Asch 2004). Uncertainty in risk prediction is a fundamental problem with when dealing with complex and chaotic systems (e.g. Keiler *et al*., 2010), this can however, be overcome through obtaining large databases and inventories (e.g. Dai *et al,* 2002); thus statistically constraining the uncertainty.

This paper describes the development of a new landslide inventory collated for the Alps based on the compilation of existing datasets in this region. The aim of this inventory is to include, where possible, the date of landslide occurrence, location and an indication of size in order to gain both a regional-scale picture of landsliding across the Alps and a perspective of the frequency and magnitude of these over time. This regional-scale inventory (RI) allows for the interrogation of landslide risk over a wide range of geologies and topographies. The temporal distribution of landslide recording will firstly be assessed, with gaps and breaks in the RI being highlighted and discussed. We then assess landslide frequency-size distributions, for both the RI and individual databases, testing the hypothesis that the log-linear relationship between landside size and frequency is present for this dataset and robust over time. We posit that these *historical* inventories can offer time-sensitive insights into how changes in the climate may affect the frequency and magnitude of landslides. Finally we discuss the representativeness of *historical* landslide inventories in Europe and prospects for future research.

2 Study region

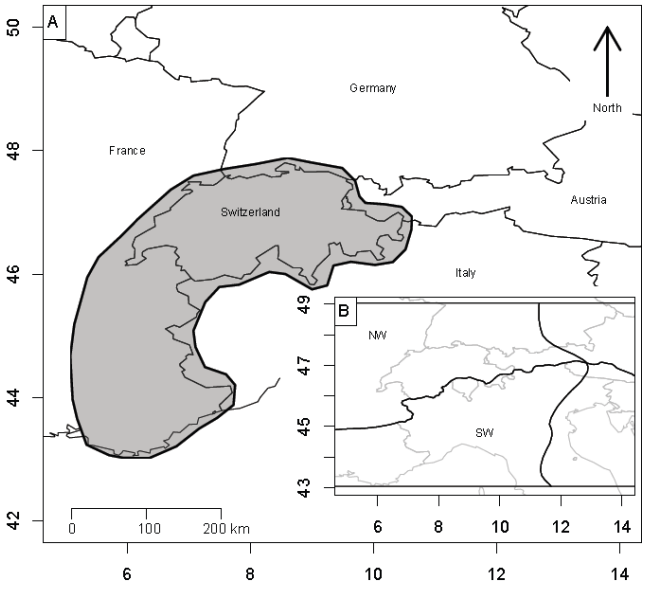

Figure 1: A: Map indicating the study site within the European Alps (grey shaded area), which includes Switzerland and South-East France. B: Showing the area covered by the north-west (NW) and south-west (SW) CRS (after Auer *et al.*, 2007, personal communication Böhm and Haslinger).

The European Alps (Figure 1) have been chosen for this study as they are amongst the most heavily developed mountain regions in the world and are affected by a range of natural hazards. Both these and the regional climate have been extensively researched (Huggel *et al.*, 2002; Schmocker-Fackel and Naef, 2010; Huggel *et al.*, 2012). This

area therefore has high potential for investigating the relationship between changing climate and natural hazards. Climatically, the Alps have been partitioned in several different ways and at different scales; for example by the influence of the North Atlantic Oscillation (Bartolini *et al*., 2009) and by differences in key climate indicators (e.g. temperature, precipitation, air pressure, etc.). Auer *et al.* (2007) distinguish four distinct climatic regions based on differences in these climatic indicators (Figure 1, insert B). These climate regimes can potentially be used by researchers to study the influence of climate on natural hazards in this region. In partitioning data by its spatial extent in this way, it is possible to negate a lack of temporal data by making links between different climate regimes in space, rather than over time.

3 Landslides

3.1.1 Classification

Classification provides a framework from which comparisons between different types of landslide at different locations can be made in order to understand common trigger mechanisms and processes involved. From a risk perspective, it is important to classify landslides by process and trigger in order to evaluate differing rates of movement which will affect mitigation and remediation works carried out to lessen potential damage caused. Precursors and trigger mechanisms vary between location and landslide class, and have been shown to increase the frequency of landsliding in certain areas due to differences in geology, lithology, topography, and terrain (Dapples *et al.*, 2002; Soldati *et al.*, 2004; Dai and Lee, 2001); thus making classification across a range of geologies and topographies paramount for the development of hazard mapping and landslide predictions.

Landslide location and velocity are the most important factors in determining landslide risk; with the two most commonly used methods of landslide classification taking specifically the latter into consideration. The first, by Varnes (1978), is the most widely-used landslide classification and is based on process, morphology, geometry, movement, rate of displacement and the type of material. These factors included in this classification allow for interrogation of the trigger mechanisms and antecedent conditions associated with the different landslide classes; particularly the inclusion of process, movement and rate of displacement. The second and more recent classification builds on the Varnes (1978) classification and additionally considers the size and rate of failure (Cruden and Varnes, 1996; Fell, 1994; Jakob, 2005). The Cruden and Varnes (1996) classification distinguishes landslides by velocity class,

while also referring to the effects of mitigation works on slow-moving slides (e.g. Velocity class 1) up to an expectation for the loss of life (e.g. Velocity class 7). Both of these methods of classification are thus important for risk assessment and hazard evaluation.

3.1.2 Landslides and climate

Recent climate change in the European Alps is manifested in fluctuations in precipitation (Casty *et al.*, 2005) and increases in temperature (Böhm, 2001; Büntgen *et al.*, 2006) leading to the loss of permafrost (Harris *et al.*, 2003) and a shift to negative glacier mass balance (e.g. WGMS, 2013). It has also been argued that the recent warming trend has influenced the "*operation of all landscape elements*" (Keiler *et al.*, 2010, p. 2462) resulting in an increase in geomorphological hazards. Alongside this, land use and vegetation change (e.g. Theurillat and Guisan, 2004), population increase and the addition of infrastructure in the European Alps (Fuchs and Bründl, 2005) has impacted geomorphological processes, leading to increased slope instability and increased risk from natural hazards such as landsliding. In order to assess which areas are affected by this increased risk, it is important to understand the role that landslides have played in the area over long periods of time, the nature of landslides, trigger mechanisms and the inclusion of regional climate predictions.

There is a considerable amount of literature on the role of temperature and precipitation change (Buma and Dehn, 1998; Collinson *et al.*, 2000; Soldati *et al.*, 2004), climate and weather variability, seasonality and storminess (Szabó, 2003; Guthrie, *et* al., 2010) and the effects of climate extremes in driving landslides. On shorter timescales, heavy precipitation leads to the initiation of shallow landslides, whilst longer-term trends in precipitation, from weeks to months, act as precursors to deep-seated landslides (Iverson, 2000; Marques *et al.*, 2008). On seasonal timescales, both freeze-thaw action and the transition between wet and dry phases vary, exaggerating mechanical weathering (Abele, 1997; Chigira, 2002). Variability and increasing temperature trends have a two-fold effect on slopes and rock walls in alpine environments; firstly by reducing the tensile and cohesive strength of rock masses resulting in a loss of stability (Chemanda *et al.*, 2005), and secondly, through permafrost degradation (Gruber *et al.*, 2004; Schär *et al.*, 2004; Harris *et al.,* 2009) increasing the potential for slope failure. Permafrost is widespread in Alpine mountains and has been affected by recent warming in the Alps (Hæberli and Beniston, 1998). The hot summer of 2003 was characterised by a 3°C rise in temperature in Switzerland, which led to both a warming of the permafrost and an increase in the depth of thaw (Gruber *et al.*, 2004). As a result, there was widespread destabilisation of rock walls

leading to increased rockfall in the region; illustrating how a short-term (seasonal) increase in temperature can have a large affect in sensitive alpine environments (Gruber *et al.*, 2004). Despite this wealth of literature discussing these factors at a large-scale, these studies cannot be up-scaled for regional hazard assessments as there is little research taking this regional-scale approach to encompass multiple landslide-affecting variables.

3.1.3 Space, time and scale

The precursors for landslides include: sediment availability, appropriate slope gradient, failure plane and appropriate antecedent conditions. The spatial distribution of landslide risk is determined both by the susceptibility of the slope and the proximity of these areas to subjects of value (such as property or infrastructure). In addition to this, antecedent conditions, trigger mechanism and topography of the region have implications for the potential runout and risk, thus scale is an important factor to consider when modelling landslide risk. A decision must be made pertaining to the scale at which these afore-mentioned factors can be realistically modelled, in order that the outputs can be deemed informative with respect to landslide predictions (e.g. Mercogliano *et* al., 2010; Hervas *et al*, 2010). Another important consideration is the scale at which it is feasible to predict landscape response to transient triggers, such as climate or weather. This in turn must be applicable to those industries for which an understanding of landslide risk is critical. The quantification of future risk lays in the consideration of these factors as an ensemble, as well as an understanding of the temporal and spatial patterns of landsliding in a region, in order to identify susceptible areas and likely triggers (e.g. Grove, 1972).

Landslides are affected by climate over a wide range of timescales, with long-term climate change (i.e. the periods between the Late glacial and the Holocene, or between the Atlantic and the Subboreal) correlating with higher frequencies of landslide activity, referred to as landslide *clusters* (Soldati *et al*., 2004). A long-term perspective of the temporal variability of transient climatic triggers (i.e. changes in temperature and precipitation indices) is required to test hypotheses made between climate and landsliding (Van Beek and Van Asch, 2004). As an example, increasing temperature and a change in its spatial pattern across the European Alps may affect the distribution of landslides through space, time and magnitude; making understanding the influence of temperature, together with precipitation, important in determining future risks posed by landslides (e.g. Marques *et al*., 2008). To fully understand and assess the time-scales at which triggers result in landslide initiation, combinations of *historical* and *modern* landslide inventories are essential.

3.1.4 Landslide inventories in Europe and their accessibility

The European Alps have been extensively studied with many academic publications investigating both individual and clusters of landslides (e.g. Nieuwenhuijezen *et al*., 1990; Couture *et al*., 1997; Bertran, 2003; Giardino *et al.* 2004; Casson *et al*., 2003; Meric *et al*., 2005; Squarzoni *et al*., 2005; Deline, 2009). More recently (in the past 20 years) landslides have been increasingly documented in European-wide inventories and databases, giving us a picture of the spatial distribution (Van Den Eeckhaut and Hervas, 2012) while also highlighting regions with high levels of landslide susceptibility. The temporal range covered by individual landslide inventories is highly variable. *Historical* inventories look at landsliding over a range of time periods including millennia to centuries (e.g. Soldati *et al*., 2004), whereas *modern* inventories tend to centre on basin-scale clusters occurring over short-periods of time, often relating to a single trigger event (e.g. Malamud *et al*., 2004). *Modern* inventories are collated in the hours, days or weeks after the triggering event, while *historical* inventories are collated over years and decades to offer a representation of the nature of landsliding in an area over time. Despite the extensive scientific research on landslides in the European Alps, data access is limited and the extraction of data from journals, printed and online media can be time-consuming, exacerbated in by a lack of detailed location data for landslides, often given at the regional level or from small-scale maps.

3.1.5 Statistics of landslide inventories

Landslides show a form of self-organised criticality whereby there is a commonality in form and process across a wide range of scales (Bak *et al*., 1987). This self-organised criticality presents itself as a log-linear trend between the frequency of landsliding and landslide area (Hergarten and Neugebauer, 1998); small landslides are represented at the high-frequency, low-magnitude portion of the distribution and large landslides by the linear, low-frequency tail (Figure 2). This relationship is commonly evaluated using *modern* landslide inventories and can be used to provide estimates for the potential of landslide occurrence in a given area, allowing assessments of statistical relationships using *modern* and *historical* landslide inventories (e.g. Stark and Hovius, 2001; Malamud *et al*., 2004). This frequency-area relationship appears to be robust and consistent across space and time (Stark and Hovius, 2001; Guzzetti *et al*., 2002; Malamud *et al.*, 2004) however, recent work has shown that this is not always the case. An example of this comes from the Maily-Say region of the Tien-Shan where, between 1962 and 2007 there was an increase in the recorded frequency of large landslides, which translated to an upward shift in the tail of the

distribution (Schögel *et al*., 2011); this was attributed to the growth of existing landslides or the coalescence of smaller landslides in the region (Torgoev *et al*., 2010). This apparent divergence from the expected distribution makes it vital to collate and update comprehensive landslide inventories for further investigations.

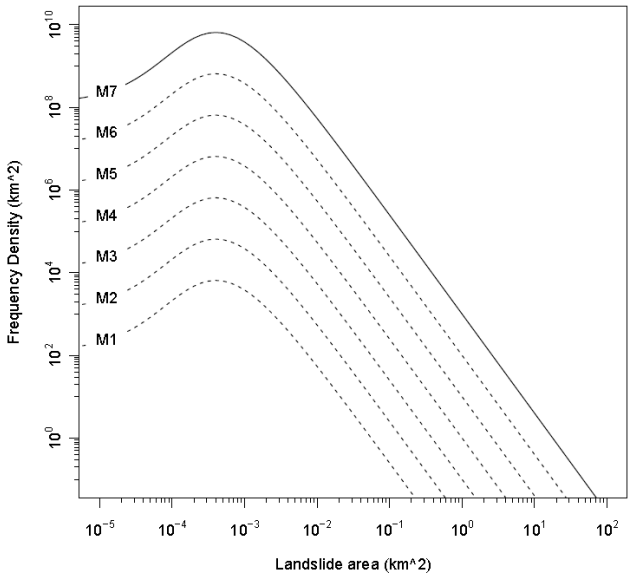

Figure 2: Theoretical landslide frequency distributions based on a three-parameter inverse-gamma distribution over a range of magnitudes (adapted from Malamud *et al*., 2004; p. 704).

Whilst landslide processes and mechanisms are understood in terms of individual landslides, recently this knowledge has been tuned to susceptibility mapping across wider areas and regions in order to better understand landslide risk (Van Den Eeckhaut *et al*., 2010; Mallet *et al*., 2010). An example of this is the *Safeland Project* which uses landslide inventories for a number of specific landslide hotspots as model validation for short-term landslide forecasting (Callerio *et al*., 2010; Mercogliano *et al*., 2010). Full exploitation of the risk management and assessment capabilities of landslide inventories requires data appropriate to the application of inventory statistics and susceptibility mapping. For wider analysis, date, location, size and the type of landslide must be routinely recorded, while failure to discriminate between different landslide classes restricts investigations into trigger mechanisms and long-term trends (Figure 3). This is easy for modern landslide inventories however, *historical* inventories cover wider areas and regions and these indicators are highly variable through space and time. This wide range of landslide-influencing factors (which also include topography and geology) need to be organised and recorded in a standardised format to ensure that all relevant data are included (see Figure 3).

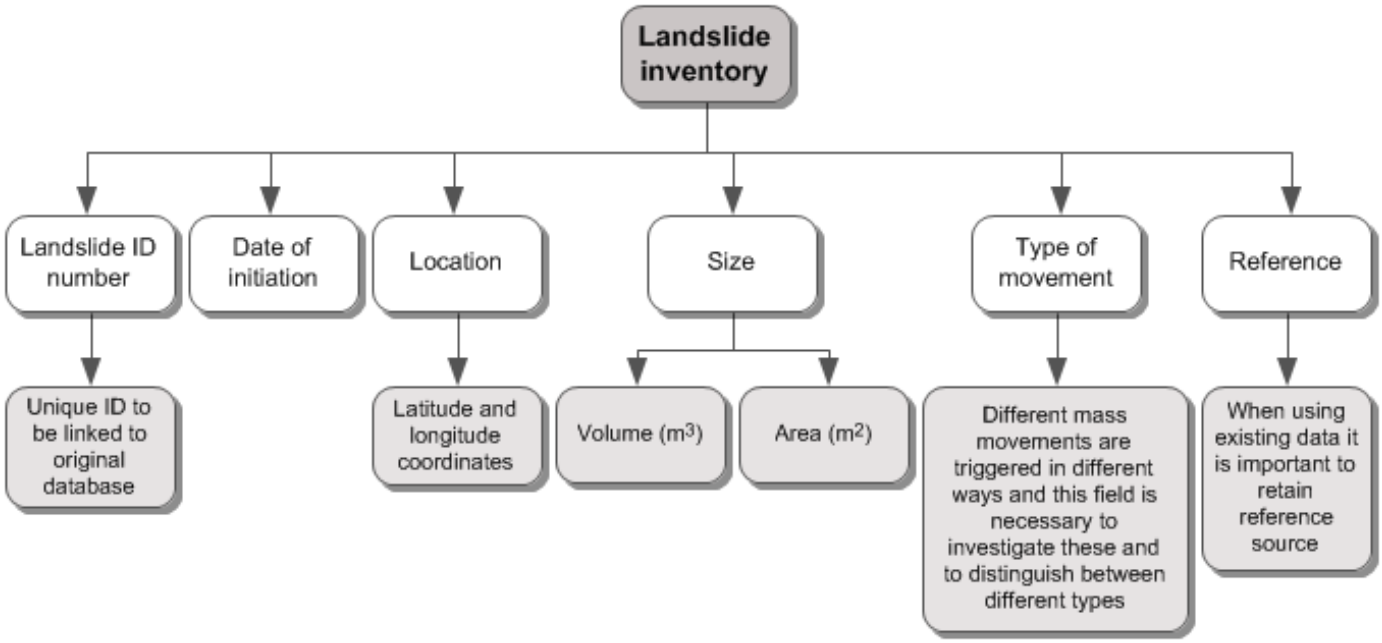

Figure 3: Flow diagram showing the required components for a *complete* landslide inventory as a tool by which to both standardise inventories compiled from different sources and for susceptibility, hazard and risk investigations.

4 Material and methods

4.1.1 Landslide Databases and Inventories in Europe

A unified database, the RI, was created in order to address the afore-mentioned issues (section 3.1.5) with landslide inventories. It was compiled from 6 existing databases together with academic publications (Table 1) with an aim to consistently record important information (from Figure 3), maintained in a unified language from the individual databases. The identification number (ID) for each landslide was maintained from the original source, and additionally assigned a new ID for the RI. The locations of all landslides within the individual databases were converted from the countries own coordinate reference system to latitude and longitude coordinates (EPSG: 4326) using a Python script in Linux. The spatial distribution of the RI is highlighted in Figure 4, with recorded characteristics shown in Table 2. Some databases included an *information* column which was explored, translated and information extracted, (particularly the size of the landslide) to the appropriate columns within the RI. In addition to this a *literature search* was carried out for academic sources, and Google Earth used as a mapping tool for this academic portion of the RI; these were exported from Google Earth as Keyhole Markup Language (.kml) files to Quantum Geographic Information Systems (QGIS) whereby the location was imported into the RI.

Table 1: The sources used to create the RI were from online databases, research institutes and academic literature. Those used in the RI predominantly covered the Swiss and French Alps. This table highlights the sources, country of origin, and their contribution to the RI (% and *n*).

	Source	Country	Contribution to inventory (%)	*n*
National database (Online)	French National Database of the Bureau de Recherches Géologiques et Minières (2013a; henceforth **BRGM**).	France	48.4	3836
	Geologische Bundesanstalt (2013; henceforth **GB**).	Austria	1.1	85
Research institutes	Swiss Flood and Landslide Damage Database of the Swiss Federal Institute for Forest, Snow and Landscape Research (henceforth **WSL;** Hilker, N., personal communication)	Switzerland	41.5	3288
	Service de Restauration des terrains en Montagne de l'Isere, Grenoble, France (henceforth **RTM**; Helmstetter, A., personal communication)	France	1.4	113
Academic sources	**Barcelonnette database** (part of the Safeland Project; Mallet, J.-P., personal communication)	France	4.1	324
	Abele (1974, henceforth **Abele**; Korup, O., personal communication)	Europe	3.3	264
	Bertran (2003)	France	0.2	1
	Casson *et al*. (2003)	France		1
	Couture *et al*. (1997)	France		4
	Deline (2009)	France		3
	Meric *et al.* (2005)	France		1
	Nieuwenhuijezen *et al*. (1990)	France		1
	Squarzoni *et al*. (2005)	France		1

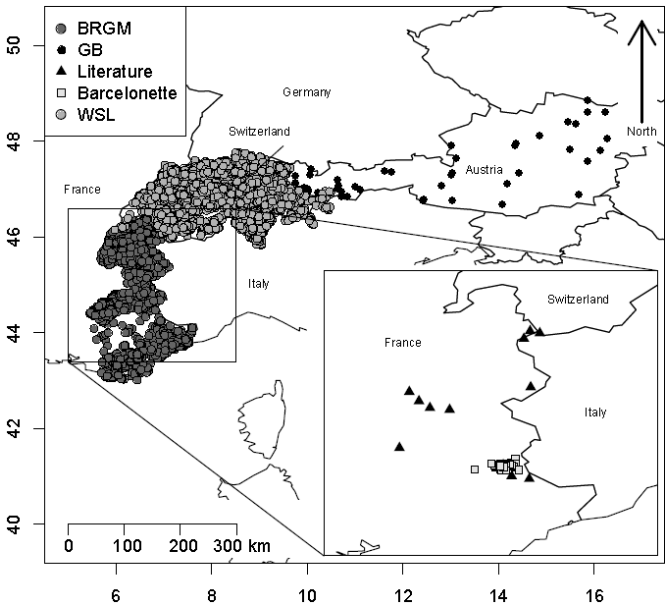

Figure 4: Locations of landslides recorded in the RI and distinguished by the contributing source (as detailed in Table 1). The insert shows the south-east region of France (excluding the BRGM, GB and WSL datasets) to show the locations of the Literature and Barcelonette datasets.

Table 2: The following table shows the attributes recorded within the RI. Those featured are considered to be key components for a *complete* landslide inventory (as detailed in Figure 3) with the addition of complimentary attributes which were available from the source datasets.

Attribute title used in the RI	Description
mvmt_cd	Code describing the classification of landslide
lat/lon	Latitude and longitude coordinates (EPSG: 4326)
crs	Course Resolution Subregion (Auer *et al.*, 2007)
ID	ID from original source
ID2	ID relating to the RI
Country	Country
Day/Month/Year	Date of occurrence
dep_ar	Area of deposit as recorded in the databases (m^2)
dep_vol	Volume of deposit as recorded in the databases (m^3)
mvmt/mvmt_cd	Description of the movement type from source / associated code
mvmt_2/mvmt2_cd	Broad classification of movement type (based on the 9 classifications) / associated code
ref	Reference for the data (academic, online reference, etc.)
slope	Angle of slope calculated in QGIS from 90m SRTM data
aspect	Slope aspect calculated in QGIS from 90m SRTM data
elevation	Elevation calculated in QGIS from 90m SRTM data
urn_litho1/2/3/4/5	Based on the BRGM geology data
L_ID/1/2/3/4	Based on Swiss Topo geology data
geology1/2	Classification of main geology type (loose sediment / sedimentary / metamorphic / igneous), based on BRGM / Swiss Topo geology data

4.1.2 Categorisation of landslides

Landslides are categorised in the RI into nine different classes (Table 3). Each individual database had its own classification system for different types of landslide and in order to distinguish these for analysis within the RI, unified definitions were created. These classifications and descriptions are based on a combination of the Varnes (1978) classification system (see also section 3.1.1), those specified within the contributing databases and are also based on the *information* and *notes* columns from each. For the purposes of the analysis of large datasets, such as the RI, a number of authors have discussed how *similarity in process* is necessary for asserting statistical assumptions across datasets, i.e. for the application of power-law statistics (Malamud *et al*., 2004; Larsen *et al*., 2010); it is for this reason that unified definitions were required (this will later be discussed in detail in sections 4.1.3 and 4.1.5).

Table 3: The following table details the different landslide classes as well as a description for each class; these were based on the Varnes (1978) classification as well as descriptions drawn from the RI sources. Finally a *name* is given describing the terms used in the RI (mvmt; Table 2), and the number of landslides in each category (*n*).

ID	Classification (translated from source)	Description	Name (material-based classification for RI)	*n*
1	Landslide	Rotational or translational landslide	*RTL*	5239
2	Rockfall landslide	Falling rocks & blocks / Sliding rock mass	*Rock*	1388
3	Rockfall / Topple	Falling/toppling rocks & blocks		163
4	Rockslide	Sliding rocks & blocks		37
5	Debris slide	Moderate to low water content / Some large particles & blocks entrained Material slides downslope	*Slides*	14
6	Mud slide	Moderate to low water content / Small unconsolidated material slides downslope		535
7	Debris flow	High water content & very liquid in movement Some large particles & blocks entrained	*Flows*	236
8	Mud flow	High water content & very liquid in movement Entrained material is fine grained (soil based)		34
9	Complex / Subsidence & collapse / Bank erosion / Creep	Combination of 2 or more classifications / Rupture of underground cavity / Erosion of banks resulting in slide / Slow gravitational creep	*Complex*	217
0	Unknown	Unspecified in the literature / database	*Unknown*	56

4.1.3 Volume-Area scaling

From the complete RI of 5239 *Rotational or Translational Landslides* (henceforth *RTL*; c.f. Table 3) recorded, only ~10% had volume data, and ~4% had area data. Larsen *et al*. (2010) show that a log-linear scaling relationship exists between area and volume for similar mass movements; this relationship was analysed for all landslide classes in the RI. For this analysis the classification of landslides (as discussed in section 3.1.1) was very important as only landslides of *similar* process are comparable. The scaling relationship was analysed for all classes of landslide individually, with an additional investigation which grouped the *RTL* and *Slide* classes (henceforth *LSS*; c.f. Table 3) being of similar process. Landslides with both area and volume data were plotted and linear models fitted (Figure 6). The scaling exponent (γ) and intercept (α) from the linear models were substituted into Equation 1 and applied to the respective classifications in the remainder of the RI (for further discussion see section 5.1.2; Figure 7).

Equation 1: Describing the volume-area scaling relationship, from Larsen *et al*. (2010, p. 247).

$$\mathbf{v} = \boldsymbol{\alpha}\, \mathbf{A}^{\boldsymbol{\gamma}}$$

where $\mathbf{v}$ = volume

$\mathbf{A}$ = area

$\boldsymbol{\alpha}$ = intercept

246 ***γ*** = scaling exponent

247 *4.1.4 Temporal recording of landslides in the RI*

248 The temporal range of the RI was investigated in order to understand how the frequency of recording has changed
249 over time. The cumulative frequency of landslide occurrence, for each database, was calculated at annual resolution
250 and both linear and *segmented models* (Muggeo 2003, 2008) were applied to the data to test for breaks in linear
251 trends. These distributions were additionally partitioned by landslide classification (c.f. Table 3) to determine
252 whether the different classes have been consistently recorded through time and between the source datasets.
253 Breaks in the *segmented models* are taken to represent periods in time at which there has been a change in the
254 recording frequency of the different landslide classes.

255 *4.1.5 Power-law distribution*

256 The frequency-area distribution is often used to quantify the completeness of a modern inventory and has been
257 shown to follow a number of different empirical distributions including double Pareto (Stark and Hovius, 2001) and
258 an inverse Gamma distribution (Malamud *et al.*, 2004; Figure 2); all exhibit a negative power-law relationship in the
259 tail of the distribution. Given the robustness of this empirical distribution and its applicability across a range of
260 triggers and geologies a series of theoretical three-parameter inverse gamma distributions (Figure 2; Equation 2)
261 were created across a range of magnitudes (after Malamud *et al*., 2004) to assess the completeness of the RI (based
262 on the areas summarised in Table 5. The frequency density for *LSS* were then calculated from Equation 3 and
263 plotted against the theoretical distributions; if we assume that the theoretical distribution is valid for the given
264 datasets in the RI then we can calculate the total landslide area (Equation 4).

265 **Equation 2: The three-parameter inverse-gamma distribution for landslide inventories (Malamud *et al*., 2004, p. 694).**

$$\boldsymbol{p(A_L;\ \rho, a, s) = \frac{1}{a\Gamma(\rho)}\left[\frac{a}{A_L - s}\right]^{\rho+1} exp\left[-\frac{a}{A_L - s}\right]}$$

266 where a = location of maximum probability

267 $\Gamma(\rho)$ = gamma function of ρ which controls the power-law decay

268 s = parameter controlling exponential rollover for low area values

269 A_L = landslide area

Equation 3: From Malamud *et al*., (2004, p. 703), calculating the frequency density of landslide area for incomplete inventories.

$$f(A_L) = \frac{\delta N_L}{\delta A_L} = N_{LT} p(A_L)$$

where $f(A_L)$ = frequency density of landslide area

$\frac{\delta N_L}{\delta A_L}$ = δN_L being the number of landslides between A_L and $A_L + \delta A_L$

N_{LT} = number of landslides in inventory

pA_L = Probability density for landslides of size A_L

Equation 4: Adapted from Malamud *et al*. (2004) to calculate the total area affected by landslides based on the maximum magnitude recorded in an incomplete inventory.

$$L_{Ta} = \left(\frac{a}{\rho - 1} + s\right) 10^{ML}$$

where L_{Ta} = total area affected by landslides

ML = maximum landslide magnitude

5 Results

5.1.1 The Regional Inventory

The databases collated for this inventory include, where possible, all of the elements specified in Figure 3. The RI contains a total of 7919 landslides, of which 56 remain unclassified, 5239 are *RTL*, 1588 are *rockfalls*, *rock slides* and *rock topples*, 549 are *debris*- or *mud-slides*, 270 are classified as *debris* or *mud flows*, and 217 are *complex* landslides (see Table 3 for details). For area and volume data the main addition to the RI came predominantly through extracting data from the *information* sections of the source datasets; leading to the addition of 525 area/volume estimates for the WSL database, 15 from the GB (through the available online literature), 10 for the Barcelonnette database, 10 were extracted from the academic publications, while 265 were digitised from Abele (1974).

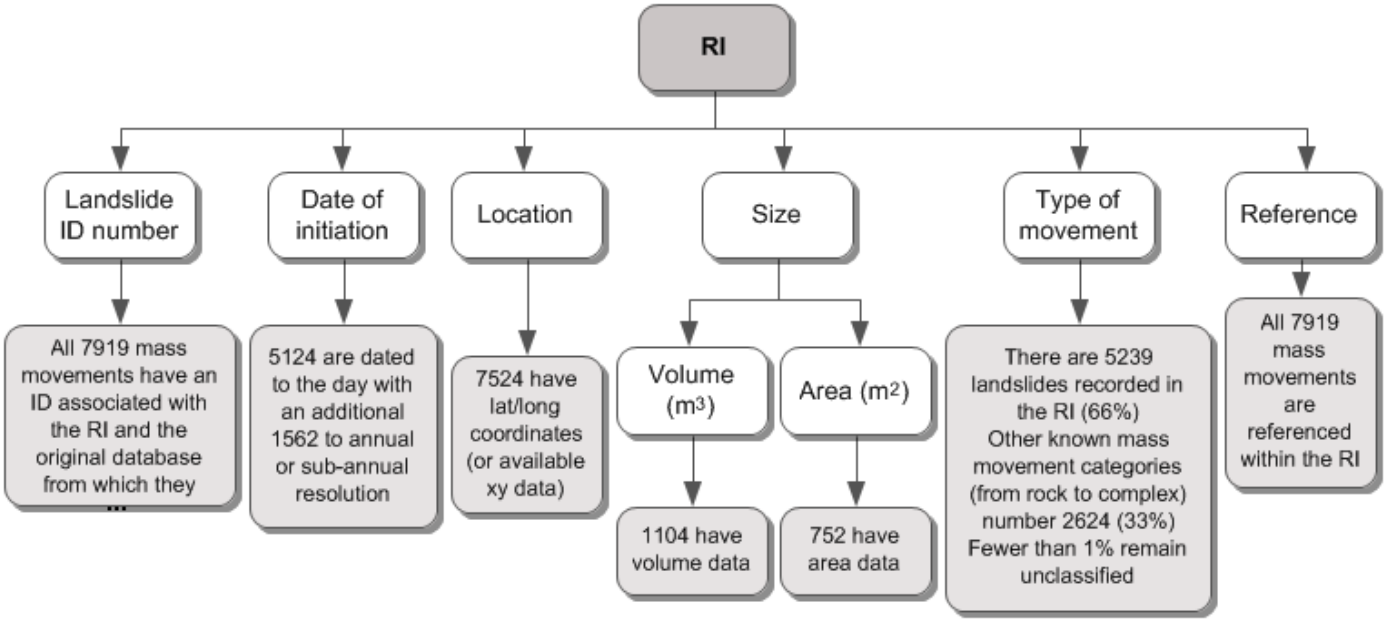

289

290 **Figure 5: Flow diagram showing the completeness of the required fields within the RI (based on Figure 3).**

291 ### *5.1.2 Volume-area scaling*

292 The relationship between area and volume was investigated for all classes of landslide in the RI; this was carried out
293 to define the scaling exponents (after Larsen *et al.* 2010) to calculate area for the landslides in the RI which only had
294 a given volume. The separate landslide classes were analysed individually as they represent different types of
295 movement with potentially different scaling relationships. Due to the low number of recorded values for *Rock*, *Slide*,
296 *Flow* and *Complex* failures (Figure 6), the exponents from the fitted linear models are inappropriate for application
297 to the remainder of the database, conversely, there were 83 *RTL* with both area and volume data. The analysis of
298 *RTL* showed an expected strong positive correlation between area and volume with R^2=0.922, γ=1.386±0.045 and
299 $\log_{10}(\alpha)$=-0.985±0.248 (Figure 6). A total of 3 *Slides* with area and volume data were considered in addition to *RTL*
300 (*LSS*) as these classes represent similar physical mechanisms and so, constitute a sensible comparison; with R^2=0.923,
301 γ=1.378±0.043 and $\log_{10}(\alpha)$=-0.941±0.239 (see Table 4 and Figure 6).

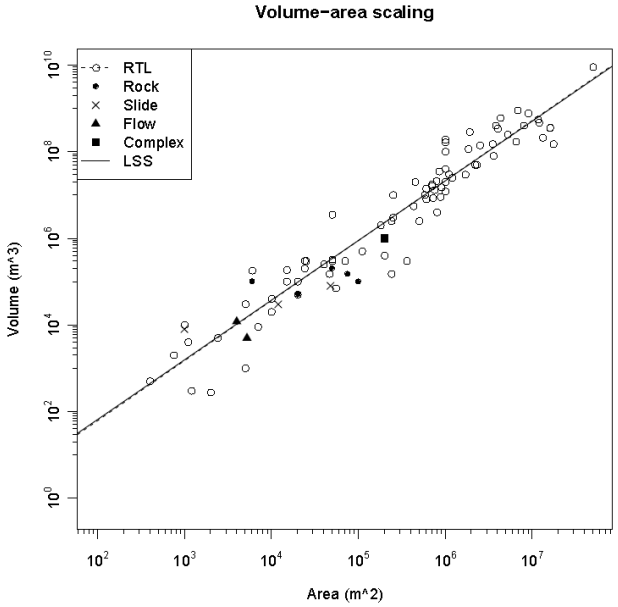

Figure 6: Showing the log-linear relationship between area and volume which exists for *RTL* and *LSS* (R^2 = 0.92 for both). The scaling exponents (γ and α) are given in Table 4. Also shown are *Rock, Slides, Flows* and *Complex* movements for which both area and volume data were available; due to the limited number of points in these classes, no linear model was fitted to these.

Table 4: This shows the estimates of γ and $\log_{10}(\alpha)$ (± the standard error for each) attained from each source for *RTL* and *LSS*. The R^2 statistic for the fit of the linear models and the number of landslides used (*n*) are also shown. These are displayed along with the Larsen *et al*. (2010) results of the scaling exponents from investigations of combined datasets; see Larsen *et al*., 2010, supplementary information for full details.

	Source	γ	$\log_{10}(\alpha)$	R^2	*n*
RI	Abele (*RTL*)	1.359±0.100	-0.776±0.625	0.80	50
	WSL (*RTL*)	1.233±0.116	-0.394±0.506	0.78	34
	All (*RTL*)	1.386±0.045	-0.985±0.248	0.92	84
	All (*LSS*)	1.378±0.043	-0.941±0.239	0.92	87
Larsen *et al.* (2010)	*Global landslides (all)*	*1.332±0.005*	*-0.836±0.015*	*0.95*	*4231*
	Soil landslides	*1.09 to 1.40±0.02*	*-1.48 to -0.37±0.06*	*0.81 to 0.95*	*11 to 956*
	Mixed soil & bedrock inventories	*1.36±0.03 to 1.450*	*-1.131 to -0.59±0.03*	*0.88 to 0.98*	*201 to 677*
	Bedrock landslides	*1.34±0.02 to 1.92±0.48*	*-4.09±3.24 to -0.49±0.08*	*0.58 to 0.98*	*11 to 140*
	Bedrock landslides (Alps & Apennines)	*1.60±0.07*	*-2.36±0.45*	*0.82*	*87*

The values attained for *RTL* and *LSS* are comparable to the range of values obtained by Larsen *et al*. (2010; Table 4 and Figure 7). As the *RTL* in the RI are *undifferentiated* (in terms of the material transported) it follows that the linear model obtained in this study would fall within the bounds of both mixed and soil inventories reported by Larsen *et al*. (2010). The RI linear model is closest to the lower bound of the mixed inventories, suggesting that soil *RTL* may be the dominant type for which area and volume data are more frequently recorded in the RI.

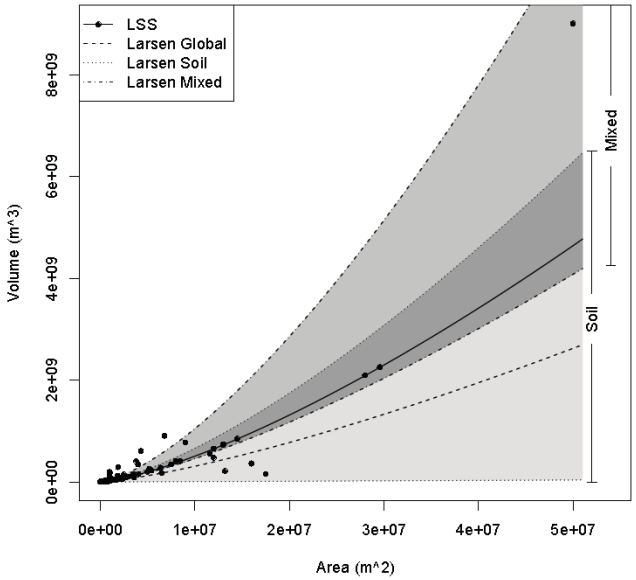

316

317 **Figure 7: The power-law statistics (see section 4.1.5) require area data for a given landslide and in order to achieve this for**
318 **the RI, the scaling relationship between area and volume was investigated for *LSS* with both area and volume data. This**
319 **figure shows the relationship (solid line), with the points representing both calculated and given area and volume data within**
320 **the RI; more than doubling the number of areas available. The scaling relationship, shown here, is compared to data derived**
321 **from Larsen *et al.* (2010) for global, soil and mixed inventories; this shows that the estimations of scaling exponents derived**
322 **for the RI are reasonable in relation to other studies. The light grey shading highlights the range of "soil", the darker grey**
323 **highlights the range of "mixed", with the darkest grey showing the overlap between the two (after Larsen *et al.*, 2010).**

324 **Table 5: The number of *LSS* (*n*) given in each source dataset and the associated range of areas (m²) for each; both before (pre**
325 **AV scaling) and after (post AV scaling) the application of the scaling relationship.**

			Pre AV scaling		Post AV scaling		
Source	**Given areas (n)**	**Calculated areas (n)**	**Min area (m²)**	**Max area (m²)**	**Min area (m²)**	**Max area (m²)**	**Temporal range**
Abele	132	16	55,000	50,000,000	55,000	50,000,000	-
Barcelonette	0	5	-	-	20,502.24	493,301.99	1898 to 1989
BRGM	0	70	-	-	2.91	493301.99	1948 to 2002
Literature	2	0	500,000	1,100,000	500,000	1,100,000	-
GB	0	9	-	-	500.18	2381477.72	1804 to 2010
WSL	74	380	100	1,000,000	7.96	1,000,000	1972 to 2010
Total	**208**	**480**					

326

327 ### *5.1.3 Temporal range and landslide recording*

328 The temporal resolution of the RI as a whole is highly variable, with some of the oldest landslides being dated to
329 1248 A.D. (in the BRGM and RTM databases) and 1451 A.D. (Barcelonnette). Despite this long record, the frequency
330 of recording prior to the 1970s is relatively low, with a sharp increase at this time. For example in the BRGM
331 database there were 589 landslides recorded between 1248 and 1969, and 2511 for the period 1970 to 2010 (Figure

8). *Segmented* linear models fitted to cumulative landslide frequency data for the BRGM and Barcelonette datasets show how recording frequency has not increased linearly through time (Figure 8). Conversely, the *RTL* and *complex* classes in the relatively short WSL dataset (from 1972) best fit a simple linear model, suggesting this database has been consistently recorded over time (Figure 8; see also Table 6).

Table 6: Results from the *segmented models* highlighting the timing of the model breaks; shown by source dataset, for each classification of landslide. Highlighted breaks are those indicated by dashed lines in Figure 8. *RTL exc. gives the output of the *segmented models* in which anomalously high frequency landslide years were excluded (in the case of the BRGM these were 1990, 1994 and 2000, and for the WSL these were 1999, 2002 and 2005; see Figure 8).**

Name (cf. Table 3)	BRGM *breaks*				Barcelonnette breaks		WSL breaks	
RTL	1772	1929	1971	1988	1937	1972	1999	
*RTL exc.**	1922		1972		-		1993	
Rock	1782	1922	1973	1986	1849		-	
Slide	1938		1981		-		-	
Flow	-				1828	1982	1988	2004
Complex	1898	1972		1989	-		1995	

In all cases the *segmented models* provide a better fit than the linear models as changes in recording frequency are clearly detected (Table 6 and Figure 8). A number of years with anomalously high frequencies of landsliding occur in the latter portion of the record in the BRGM (1990, 1994, and 2000) and WSL datasets (1999, 2002 and 2005); these were removed to test their influence on the *segmented models*. Following the removal, the BRGM dataset showed an earlier linearity and consistency in recording, from 1972 onwards as opposed to 1988, for *RTL*. In the case of the WSL dataset, although the removal of these *high frequency years* resulted in an earlier break year of 1993, the linear model provides a good fit to the data suggesting consistent landslide recording from the outset (Table 6). The changes observed in these years require further analysis to determine the cause of such a sharp increase in the numbers of observed landslides. Considering the landslide classes individually, there is a disparity in the recording both within and across the respective source datasets; with differences in the frequency of recording between the different classes of landslide within each dataset. In the case of the BRGM dataset, landslide recording was low prior to the 1940/50's and this is consistent across all classes, with the exception of *complex* which did not see an increase until 1989. *Slide* and *complex* classes are not well documented in this dataset however, this is possibly due to discrepancies between terminology used at different times. For the Barcelonette dataset *flows* are the most commonly recorded class which is evident particularly when compared with the number of *RTL* and *rock classes* in this dataset (Figure 8). *Rock* landslides in this dataset show a linearity in recording from 1849, which is much lower

than the other classes in this dataset; being 1972 for *RTL* and 1982 for *flows*. The WSL is maintained for the purpose of insurance and could be biased towards certain landslide classes which are more damaging, fast-flowing or less easy to predict or mitigate; these may naturally be more prevalent in this type of database. For this dataset, *RTL* are the most common class, with *complex* and *flows* making a small proportion of the data, only being recorded from 1980 and 1978 respectively. It is clear from this that the different classes are not being recorded simultaneously within the datasets, and this is potentially an issue for analyses attempting to understand changes in these over time.

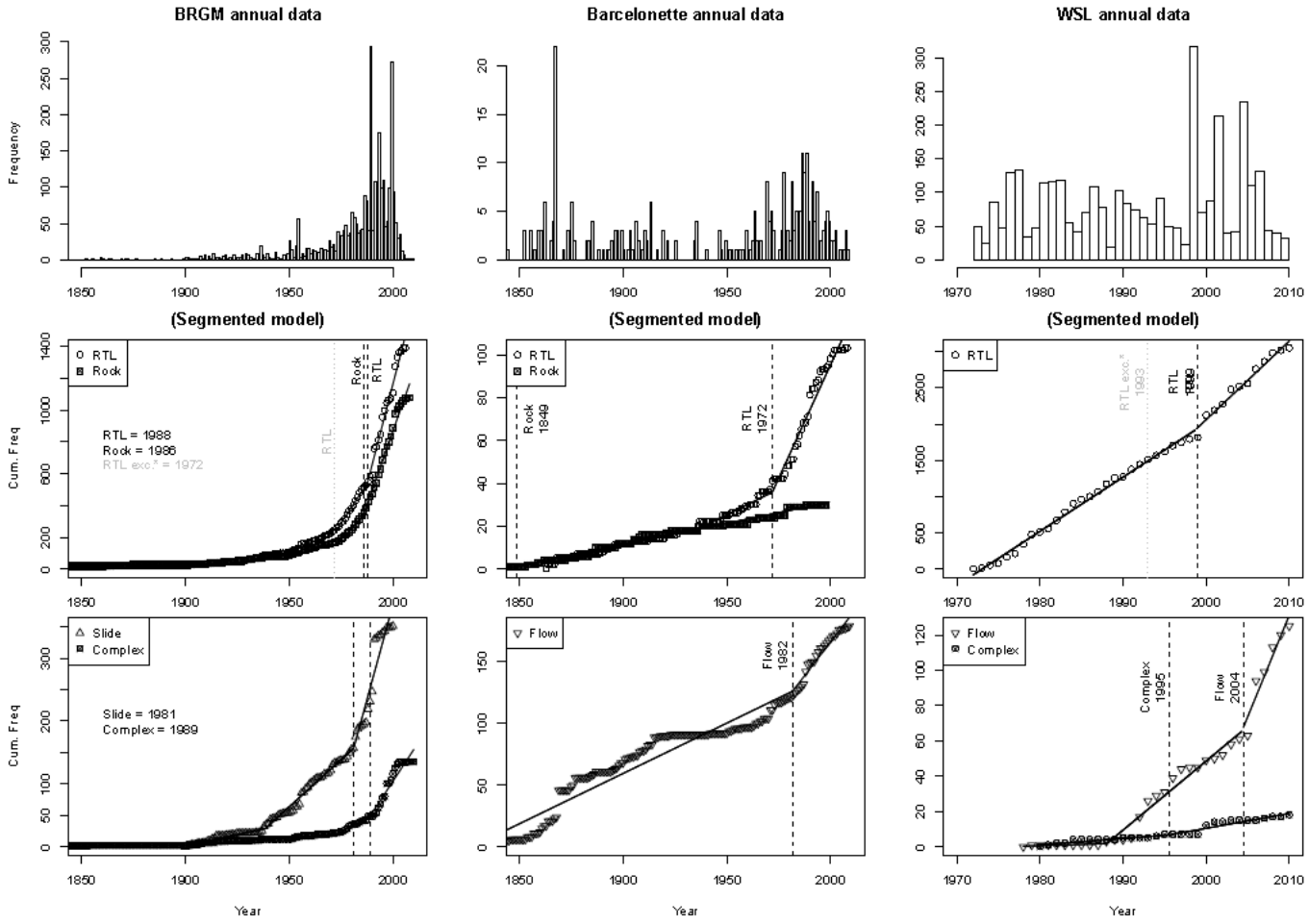

Figure 8: Temporal distribution of the three main contributors to the RI at annual resolution. (Top) Histograms of each dataset, for all landslide classes. (Middle & bottom) Cumulative distributions of different landslide classes; each fitted with a linear segmented model (Muggeo 2003, 2008) to highlight breaks in data recording. All show the timing of the last break for each landslide class (given in Table 6; dashed black line). The segmented model for the BRGM and WSL *landslide* classes were recalculated, omitting anomalous years (as per discussion in this section), the last break from these are also included (RTL exc.*; grey lines).

5.1.4 Power-law distribution

The area-frequency distributions were created following the volume-area scaling using data set out in Table 5. *RTL* and *slides* (*LSS*) were combined as they represent *similar physical mechanisms*; Malamud *et al*. (2004) noted that differences in process associated with different landslide classes affect the area-frequency statistics, for example, they have shown the distribution of rockfalls has a simple log-linear trend without an exponential rollover, as is observed for *RTL* distributions. The analysis shows that the data collated for the RI fit a range of theoretical magnitudes from 2 to 7 (Figure 9), potentially due to the use of a number of different datasets in the compilation. Analysis of the main contributors to this distribution (Figure 10) show that the Abele dataset, which includes the largest *LSS* recorded in the database, is causing the upwards shift in the tail from around 10^0 km^2. The WSL dataset only crosses two magnitudes (from 2 through to 4) and best fits the log-linear tail of the theoretical relationship, although the slope of the line is less than that of the theoretical distribution (Figure 10). All datasets exhibit an exponential-*type* rollover between $10^{-4.5}$ and 10^{-4} km^2, which is lower than that of the theoretical distribution, occurring at ~10^{-3} km^2 (Figure 9 and Figure 10). The distributions for the RI, BRGM and WSL, while exhibiting an exponential rollover and a log-linear tail, are underrepresented by medium-sized *LSS* (between 10^{-4} and 10^{-2} km^2). Conversely, the Abele dataset is centred on recording large landslides in the Alps and expectedly underrepresents small- to medium-sized *LSS*.

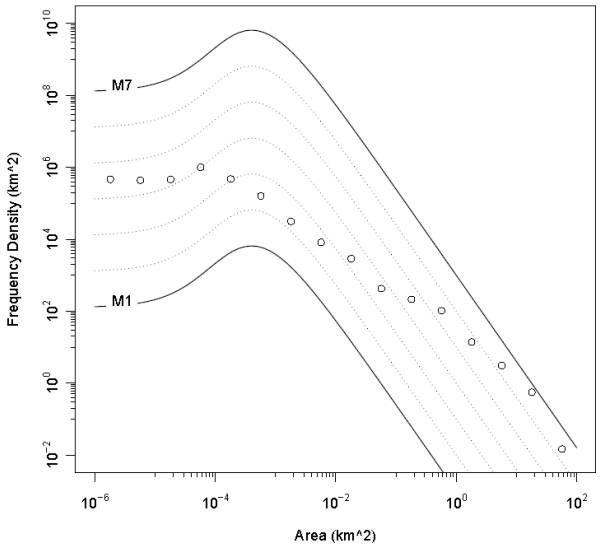

Figure 9: Showing the theoretical three-parameter inverse-gamma distribution across a range of magnitudes (Equation 2) with calculated *LSS* frequency density (*n* = 688; Equation 3).

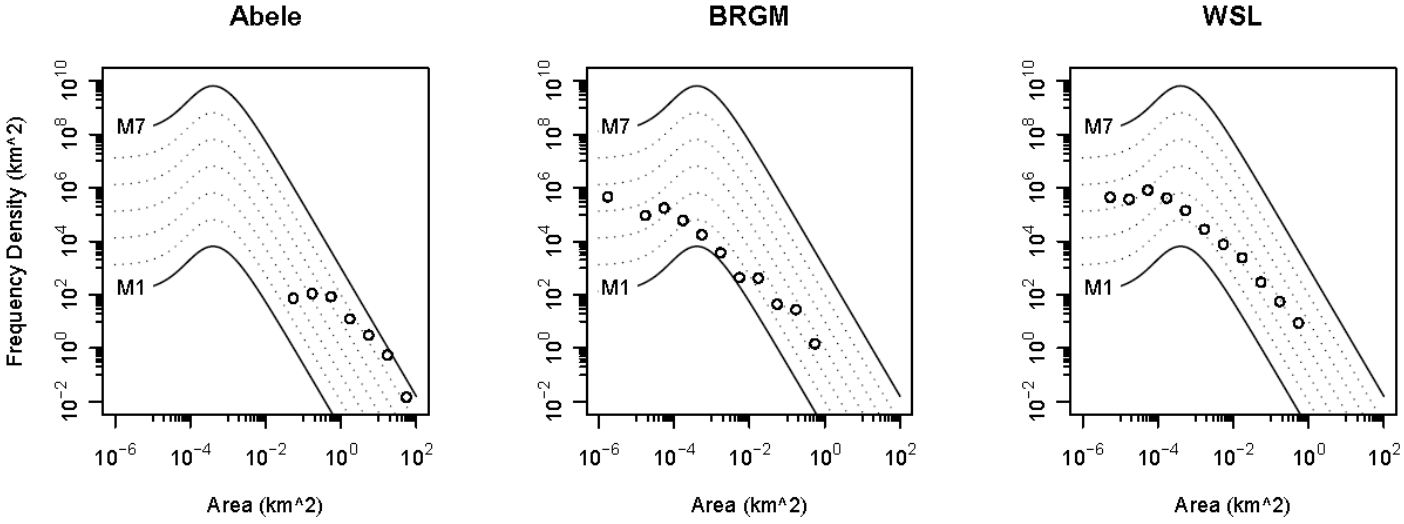

Figure 10: Three-parameter inverse-gamma distributions for calculated *LSS* frequency densities for the Abele (*n*=148), BRGM (*n*=70) and WSL (*n*=454) datasets.

Table 7: Table showing the total *LSS* area recorded in the RI for each of the individual sources. Maximum magnitude was used to estimate the total area affected by *LSS* (based on Equation 4) as the area-frequency distribution is shown to be robust for the RI and therefore *LSS* area is unlikely to be over-recorded. The percentage of data estimated as *missing* is calculated from the discrepancy between recorded and estimated areas.

	Source	Total area recorded in RI (km^2)	Minimum magnitude	Maximum magnitude (ML)	Mean magnitude	Total estimated area (km^2); Equation 4	Data missed from RI (%)
All years & undated	RI (all)	480.95	2.26	6.74	4.34	16948.18	97.16
	Abele	461.60	2.87	6.74	5.36	16948.18	97.28
	BRGM	1.75	1.33	4.52	2.72	102.00	98.29
	WSL	9.57	2.21	4.41	3.42	79.28	87.93
Post 1972	RI (all)	15.11	2.25	4.56	3.56	112.50	86.57
	BRGM	1.42	1.27	4.56	2.45	112.50	98.74

Only considering data in the *complete portion* of the RI (i.e. post 1972 for *LSS*) improves the consistency of the RI data across the magnitudes compared with all RI data (Figure 10 and Table 7). The Abele dataset is automatically excluded as this portion of the RI is part of the undated ~15% (Figure 5), while the WSL dataset is not affected as this it was recorded from 1972. The analysis of this portion of the RI therefore consists of mainly the WSL and BRGM datasets. Including only dated *LSS* results in an increase in estimates of completeness for the RI; partly influenced by the reduction of the estimate of magnitude (Table 7). The low magnitude range shown for the post-1972 RI (Table 7

Table 7) implies that this portion of time fits most consistently with the theoretical distribution however, while this portion of the RI more closely fits the theoretical distribution, there is an under-recording of *LSS* in the range 10^{-4} to

404 10^{-1} km^2 (Figure 11). Along with the WSL data, the post-1972 RI data show the lowest ranges in magnitude while
405 there is little change between the two estimates of magnitude for the BRGM (Table 7).

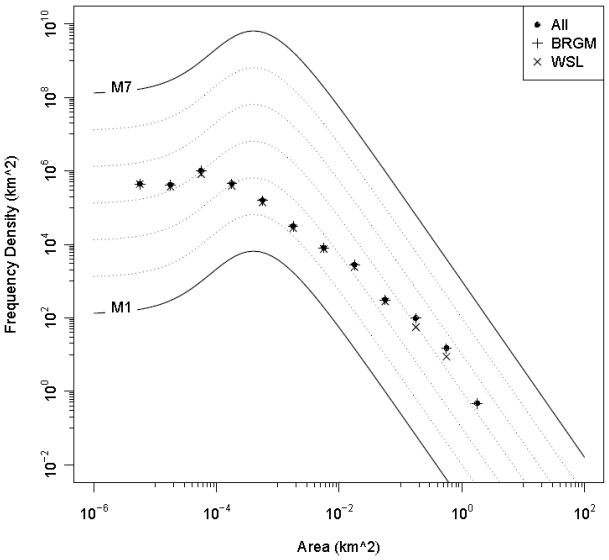

406

407 **Figure 11: Showing the area frequency distribution for the post-1972 RI, BRGM and WSL datasets (for *LSS*). We estimate for**
408 ***LSS* in the RI that between 86% (post-1972) and 97% (for *all* dates) of the area data are missing (Table 7).**

409 # *6 Discussion*

410 ### *6.1.1 The Regional Inventory*

411 We compiled an inventory (RI) of 7919 landslides in the European Alps; encompassing a range of landslide classes.
412 Several of the databases used omitted a large proportion of important landslide elements such as magnitude,
413 velocity and timing of failure, which are commonly recorded in *modern* databases (Sorriso-Valvo, 2002). We
414 included these metrics where possible however, recording of such data is inconsistent. For example the BRGM
415 include a category for landslide volume (m³), yet only 7.5% of 3836 (a total of 289) landslides downloaded for the RI
416 included volume data. Despite these discrepancies, the post-1972 portion of the RI follows the theoretical frequency
417 distribution (Figure 11) and is arguably representative of the region.

418 There is little consistency in recording different types of landslide across the RI through time (Figure 8). If we assume
419 that a linear fit to the cumulative frequency of different landslide classes over time means that there is uniformity in
420 recording, then we might expect to see the different datasets recording similar proportions of each class at similar
421 times. This would result in consistent breaks across all landslide classes in the segmented models (Table 6 and Figure

8) however, this does not happen across all databases. Reasons for this may include that over the long temporal record of the RI, definitions have changed or there have been changes in how landslides are recorded. This premise cannot be fully tested at this stage as only the relatively short WSL dataset allows for this further interpretation of landslide classes (mvmt2/mvmt2_cd; Table 2) due to there being additional notes which include descriptions of the event. To align the RI with the classes defined in Table 3, a number of the landslides in the WSL were re-defined however, from this, a recording bias due to a change in definitions was not apparent over time.

A self-similar scaling relationship exists between landslide area and frequency, which manifests a log-linear trend in the tail of the power-law distribution; we have demonstrated that this relationship is present for *RTL* in the RI dataset (Figure 9) however, contrasting approaches to database collation result in a bimodal frequency distribution for the RI (Figure 10). A post-1972 analysis shows that this portion of the RI provides the best fit to the theoretical distribution and the lowest range of magnitudes (Figure 11 and Table 7). The main contributors to this post-1972 portion of the analysis were the WSL and BRGM datasets (Figure 10). At this point the Abele dataset is omitted from analyses as landslides included in this dataset remain undated, whilst also being biased towards larger landslides (Figure 10). We highlight that a result of "*no landslides*" means that no landslide has been recorded, not that no landslide has occurred. This again potentially introduces a bias towards very large landslides (as is common in *historical* datasets) and towards those which have resulted in damage to life, infrastructure and property. The WSL, being an insurance inventory, only records landslides when a claim is made however, *RTL* recorded in this portion of the RI best represent the theoretical three-parameter inverse-gamma distribution (Table 7). In all cases, for the post-1972 portion of the RI, *RTL* between 10^{-4} and 10^{-1} km^2 are under-recorded (Figure 11) however, the compilation of different datasets still provide a robust and comprehensive inventory, closely matching the theoretical; we deduce that this portion of the RI is therefore applicable for use in susceptibility studies and hazard assessments.

6.1.2 Consistency between inventories

The format of each of the available online databases differs as each is maintained by different organisations. For instance, the interface of the online GB database involves using links to both academic and internet-based publications; requiring methods of extraction similar to that of the *literature search* (c.f. section 4.1.1). Conversely, the BRGM has a user-friendly interface, whereby data can be downloaded individually or by region to a Comma

Separated Value (.csv) or Microsoft Excel format. Differences in language and classification schemes between inventories also reduce comparability, specifically the terms used in each to describe different classes of landslide. The WSL dataset for example, does not discriminate between *RTL* and saturated or hyper-concentrated *flows*, although the trigger mechanisms differ; this lack of discrimination reduces the applicability of the dataset for climate change research as distinctions between these are vital in understanding relationships between cause and effect. This reinforces the need for a unified classification system such as that developed for the RI. Construction of a regional scale inventory is difficult due to these differences in language, terminology and data access across the Alps, supporting the need for interdisciplinary and international collaboration to develop and maintain such datasets in a unified language amongst different agents across the Alps and Europe.

In the past it has been difficult to attribute changes in the frequency of landsliding to climate change as the recording of landslides through time has been inconsistent (Figure 8). This lack of consistency in recording of the data restricts attempts to attain a long-term perspective on the frequency of an event, as it can be difficult to distinguish a real increase in frequency from an increase in recording frequency. The temporal range of the RI is relatively short in terms of the *well-documented* (i.e. post-1972) portion of the dataset (Figure 8). Breaks in the temporal record were identified for the RI by the application of the segmented model (Table 6 and Figure 8). These breaks could arise due to a number of factors including land-use change, mitigation works, inconsistencies in recording, and changes in people's perception of risk. The BRGM dataset began development in 1994 (BRGM, 2013b) and one might expect to see an increase in the frequency of recording after this time as a result however, this is not reflected in the breaks seen in the dataset, suggesting that the dataset is affected by other unidentified influences. These all serve to obscure relationships between landslides and climate change however, we have shown that creating a unified database (RI) can increase the reliability of identification of these breaks and consistency in recording.

7 Conclusion

Landslide inventories and databases have the potential to enable us to develop a better understanding of landslide patterns across regions and through space and time. These preliminary analyses of a newly collated database for the European Alps demonstrate the potential information which can be drawn from a variety of sources. As the RI is by

no means exhaustive, we hope that this highlights the need for collaboration between researchers and agencies across the European Alps. With increased input and research into these collations, a greater understanding of the observed spatial and temporal patterns of landsliding can be gained. A number of publications (e.g. Soldati *et al.*, 2001) have distinguished changes in the climate as being influential in determining the occurrence of landslide clusters. Therefore, greater emphasis on extending records back through time and improving *historical* datasets in the European Alps is important for attributing changes in landslide frequency and size to changes in the climate of the region. H*istorical* databases can offer insights into understanding changes in landslide size and spatial distribution through time, facilitating future research and predictions in regions such as the Alps for the insurance market and for policy makers.

The primary aim of this research was to construct a unified database for the European Alps to include both long-term records and all relevant metrics (Figure 3) to enable a clear indication of the spatial and temporal patterns of landsliding over the 20th Century. Our results show that we were successful in this for the post-1972 portion of the data; firstly through the evidence from the power-law distributions (Figure 9 and Figure 10) and secondly from the use of segmented models (Figure 8). This shows that it is possible to improve records by collating and analysing existing datasets; which can be greatly facilitated through interdisciplinary and international collaboration. The date of initiation, landslide size and its classification are all important metrics to be included. Current increases in temperature (e.g. Böhm, 2001; Büntgen *et al*., 2006) and precipitation variability (e.g. Casty *et al*., 2005) across the European Alps, combined with future climate projections, necessitate an understanding of the relationships between climate change and landsliding for policy makers and planners therefore, the construction of this database is an important step towards analysing this relationship and offering future predictions.

Acknowledgements

Thank you Lloyds of London for helping to fund this research. For data contribution to the RI, many thanks to J.-P. Mallet for the Barcelonnette database, to N. Hilker and A. Badoux for the WSL inventory, to O. Korup for providing the Abele dataset, and to A. Helmstetter for the RTM database. Thank you also to R. Böhm and K. Haslinger for providing the HISTALP data. Additional thanks to J. Bennie and M. Prett for providing helpful feedback.

References

Abele, G. (1974). Bergstürze in den Alpen. Wissenschaftl. Alpenvereinshefte **25**, 230.

Abele, G. (1997). Influence of glacier and climatic variation on rockslide activity in the Alps. In Matthews, J.A. , Brunsden, D. , Frenzel, B. , Gläser, B. and Weiss, M. [Eds.], Rapid mass movement as a source of climatic evidence for the Holocene, Stuttgart: Gustav Fischer Verlag, 1–6.

Auer, I., Böhm, R., Jurkovic, A., Lipa, W., Orlik, A., Potzmann, R., Schöner, W., Ungersböck, M., Matulla, C., Briffa, K., Jones, P., Efthymiadis, D., Brunetti, M., Nanni, T., Maugeri, M., Mercalli, L., Mestre, O., Moisselin, J.-M., Begert, M., Müller-Westermeier, G., Kveton, V., Bochnicek, O., Stastny, P., Lapin, M., Szalai, S., Szentimrey, T., Cegnar, T., Dolinar, M., Gajic-Capka, M., Zaninovic, K., Majstorovic, Z. and Nieplova (2007). HISTALP – Historical Instrumental Climatological Surface Time Series of the Greater Alpine Region. *International Journal of Climatology* **27**, 17-46.

Bak, P., Tang, C. and Weisenfeld, K. (1987). Self-organised criticality: An explanation of the 1/f noise, *Physical Review Letters* **59**, 381-384.

Bartolini, E., Claps, P. and D'Odorico, P. (2009). Interannual variability of winter precipitation in the European Alps: Relations with the North Atlantic Oscillation. *Hydrological Earth Systems Science* **13**, 17-25.

Bertran (2003). The rock-avalanche of February 1995 at Claix (French Alps). *Geomorphology* **54**, 339-346.

Böhm, R., Auer, I., Brunetti, M., Maugeri, M., Nanni, T. and Schöner, W. (2001). Regional temperature variability in the European Alps: 1760-1998 from homogenized instrumental time series. *International Journal of Climatology* **21(14)**, 1779-1801.

BRGM (2013a). French National Database of the Bureau de Recherches Géologiques et Minières. Available online at http://www.bdmvt.net/. Last accessed 30/11/2013.

519 **BRGM (2013b)**. Mouvements de Terrain: Objectifs et Historique. Available online at http://www.bdmvt.net/presentation.asp.
520 Last accessed 31/11/2013.

521 **Buma, J and Dehn, M. (1998).** A method for predicting the impact of climate change on slope stability. *Environmental Geology*
522 **35(2-3)**, 190-196.

523 **Büntgen, U., Frank, D.C., Nievergelt, D. and Esper, J. (2006).** Summer temperature variations in the European Alps, A.D. 755-
524 2004. *Journal of Climate* **19(21)**, 5606-5623.

525 **Callerio, A., Davi, M. and Nadim, F. (2010).** Case studies for verification/calibration of models and scenarios in the Project
526 SafeLand. In Mountain Risks: Bringing Science to Society, Mallet, Glade and Casagli (Eds.).

527 **Casson, B., Delacourt, C., Baratoux, D. and Allemand, P. (2003).** Seventeen years of the "La Clapière landslide evolution
528 analysed from ortho-rectified aerial photographs. *Engineering Geology* **68**, 123–139.

529 **Casty, C., Wanner, H., Luterbacher, J., Esper, J. and Böhm, R. (2005).** Temperature and precipitation variability in the European
530 Alps since 1500. *International Journal of Climatology* **25**, 1855-1880.

531 **Chemenda, A., Bouissou, S. and Bachmann, D. (2005).** Three-dimensional modelling of deep-seated landslides: new technique
532 and first results. *Journal of Geophysical Research* **110**, doi:10.1029/2004JF000264.

533 **Chigira, M. (2002).** The effects of environmental changes on weathering, gravitational rock deformation, and landslides. In
534 Environmental Change and Geomorphic Hazards in Forests. Sidle, R.C. [Ed.]. CABI Publishing, Oxon, UK.

535 **Collinson, A., Wade, S., Griffiths, J. and Dehn, M (2000).** Modelling the impact of predicted climate change on landslide
536 frequency and magnitude in SE England. *Engineering Geology* **55(3)**, 205-218.

537 **Couture,R., Antoine, P., Locat, J., Hadjigeorgiou,J., Evans, S.G. and Brugnot, G. (1997).** Quatre cas d'avalanches rocheuses dans
538 les Alpes françaises. *Canadian Geotechnical Journal* **34**, 102-–119.

539 **Crozier, M.J. and Glade, T. (2004).** Landslide Hazard and Risk : Issues, Concepts and Approach. In Landslide Hazard and Risk
540 (Eds. Glade, T., Anderson, M.G. and Crozier, M.J. 2004,

541 **Cruden, D. and Varnes, D. (1996).** Landslide types and process. In A. Turner and R. Schuster (Eds.), Landslides: Investigation and
542 mitigation (pp. 36– 75). Washington, DC' Transportation Research Board, National Research Council, National Academy Press.

543 **Dai, F.C. and Lee, C.F. (2001).** Frequency-volume relation and prediction of rainfall-induced landslides. *Engineering Geology* **59**,
544 253-266.

Dai, F.C., Lee, C.F. and Ngai, Y.Y. (2002). Landslide risk assessment and management: an overview. *Engineering Geology* **64**, 65-87.

Dapples, F., Lotter, A.F., van Leeuwen, J.F.N., van der Knaap, W.O., Dimitridis, S. and Oswald, D. (2002). Paleolimnological evidence for increased landslide activity due to forest clearing and land-use since 3600 cal BP in the western Swiss Alps. *Journal of Paleolimnology* **27**, 239-248.

Deline, P. (2009). Interactions between rock avalanches and glaciers in the Mont Blanc Massif during the late Holocene. Quaternary Science Reviews **28**, 1070-1093.

Fell, R. (1994). Landslide risk assessment and acceptable risk. *Canadian Geotechnical Journal* **31**, 261-272.

Fuchs, S. and Bründl, M. (2005). Damage potential and losses resulting from snow avalanches in settlements of the Canton of Grisons, Switzerland. *Natural Hazards* **34**, 53-69.

Geologische Bundesanstalt (2013). Massenbewegungen – Mass Movements. Available online: http://geomap.geolba.ac.at/MASS/index.cfm. Last accessed 31/10/2013.

Giardino, M., Giordan, D. and Ambrogio, S. (2004). G.I.S. technologies for data collection, management and visualization of large slope instabilities: two applications in the Western Italian Alps. *Natural Hazards and Earth System Sciences* **4**, 197–211.

Grove, J.M. (1972). The incidence of landslides, avalanches and floods in Western Norway during the Little Ice Age. *Arctic and Alpine Research* **4(2),** 131-138.

Gruber, S., Hoelzle, M. and Haeberli, W. (2004). Permafrost thaw and destabilisation of Alpine rock walls in the hot summer of 2003. *Geophysical Research Letters* **31**, doi:10.1029/2004GL020051, 2004.

Guthrie, R.H., Mitchell, S.J., Lanquaye-Opoku, N. and Evans, S.G. (2010). Extreme weather and landslide initiation in coastal British Columbia. *Quarterly Journal of Engineering Geology and Hydrology*, **43**, 417-428.

Guzzetti, F., Malamud, B.D., Turcotte, D.L. and Reichenbach, P. (2002). Power-law correlations of landslide areas in central Italy. *Earth and Planetary Science Letters* **195(3-4)**, 169-183.

Guzzetti, F. (2005). Landslide Hazard and Risk Assessment: Concepts, methods and tools for the detection and mapping of landslides, for landslide susceptibility zonation and hazard assessment, and for landslide risk evaluation. PhD Thesis, Bonn University.

Hæberli, W. and Beniston, M. (1998). Climate change and its impacts on glaciers and permafrost in the Alps. *Ambio* **27(4)**, 258-265.

Hæberli, W., Frauenfelder, R., Hoelzle, M. and Maisch, M. (1999). On rates and acceleration trends of global glacier mass changes. *Geografiska Annaler: Series A, Physical Geography* **81(4)**, 585-591.

Harris, C., Mühll, D.V., Isaksen, K., Hæberli, W., Sollid, J.L., King, L., Holmlund, P., Dramis, F. Guglielmin, M. and Palacios, D. (2003). Warming permafrost in European mountains. *Global and Planetary Change* **39(3-4)**, 215-225.

Harris, C., Arenson, L.U., Christiansen, H.H., Etzelmüller, B., Frauenfelder, R., Gruber, S., Hæberli, W., Hauck, C., Humlum, O., Isaksen, K., Kääb, A., Kern-Lüschg, M.A., Lehning, M., Matsuoka, N., Murton, J.B., Nötzli, J., Phillips, M., Ross, N., Seppälä, M., Springman, S.M. and Mühll, D.V. (2009). Permafrost and climate in Eeurope: Monitoring adn modelling thermal, goemorphological and geotechnical responses. *Earth-Science Reviews* **92(3-4)**, 117-171.

Hergarten, S. and Neugebauer, H.J. (1998). Self-organise criticality in a landslide model. *Geophysical Research Letters* **25(6)**, 801-804.

Hervas, J., Günther, A., Reichenbach, P., Mallet, J.-P. and Van Den Eeckhaut, M. (2010). Harmonised approaches for landslide susceptibility mapping in Europe. In Mountain Risks: Bringing Science to Society, Mallet, Glade and Casagli (Eds.).

Hilker, N., Badoux, A and Hegg, C. (2009). The Swiss Flood and Landslide Damage Database 1972-2007. *Natural Hazards and Earth System Science* **9**, 913-925.

Huggel, C., Kääb, A., Haeberli, W., Teysseire, P. and Paul, F. (2002). Remote sensing based assessment of hazards from glacier lake outbursts: a case study in the Swiss Alps. *Canadian Geotechnical Journal* **39**, 316–330.

Huggel, C., Clague, J.J. and Korup, O. (2012). Is climate change responsible for changing landslide activity in high mountains? *Earth Surface Processes and Landforms* **37**, 77–91.

Iverson, R.M. (2000). Landslide triggering by rain infiltration. *Water Resources Research* **36**, 1897-1910.

Jaboyedoff, M., Baillifard, F., Kaufmann J.F. and Labiouse, V. (2003). Identification des versants rocheux potentiellement instables. *Quanterra*, International Independant Centre of Climate Change Impact on Natural Risk Analysis in Mountainous Area. Available online at http://www.quanterra.org/Quanterra_Short_Course_3F.pdf. Last accessed 03/09/2010.

Jakob, M (2005). A size classification of debris flows. *Engineering Geology* **79**, 151-161.

Katz, R.W. and Brown, B.G. (1992). Extreme events in a changing climate: Variability is more important than averages. *Climatic Change* **21(3)**, 289-302.

Keiler, M., Knight, J. and Harrison, S. (2010). Climate change and geomorphological hazards in the eastern European Alps. *Philosophical Transactions of the Royal Society A* **368**, 2461-2479.

Larsen, I.J., Montgomery, D.R., and Korup, O. (2010). Landslide erosion controlled by hillslope material. *Nature Geoscience Letters* **3**, 247-251.

Lee, E.M. and Jones, D.K.C. (2004). Landslide risk assessment. Thomas Telford Books (Pubs.), London.

Malamud, B.D., Turcotte, D.L., Guzzetti, F. and Reichenbach, P. (2004). Landslide inventories and their statistical properties. *Earth Surface Processes and Landforms* **29(6)**, 687-711.

Mallet, J.-P., Glade, T. and Casagli, N. (2010). The "Safeland" Project: Living with landslide risk in Europe. In Mountain Risks: Bringing Science to Society, Mallet, Glade and Casagli (Eds.), p523-558.

Marques, R., Zêzere, J., Trigo, R., Gaspar, J. and Trigo, I. (2008). Rainfall patterns and critical values associated with landslides in Povoação County (São Miguel Island, Azores): relationships with the North Atlantic Oscillation. *Hydrological Processes* **22**, 478-494.

Meric, O., Garambois, S., Jongmans, D., Wathelet, M., Chatelain, J.L. and Vengeon, J.M. (2005). Application of geophysical methods for the investigation of the large gravitational mass movement of Séchilienne, France. *Canadian Geotechnical Journal* **42**, 1105-1115.

Mercogliano, P., Schiano, P., Picarelli, L., Olivares, L. , Catani, F., Tofani, V., Segoni, S. and Rissi, G. (2010). Short term weather forecasting for shallow landslide prediction. In Mountain Risks: Bringing Science to Society, Mallet, Glade and Casagli (Eds.).

Muggeo, V.M.R (2003). Estimating regression models with unknown break-points. *Statistics in Medicine* **22**, 3055-3071.

Muggeo, V.M.R (2008). Segmented: an R Package to Fit Regression Models with Broken-Line Relationships. R News, 8/1, 20-25. URL: http://cran.r-project.org/doc/Rnews/.

Nieuwenhuijezen, M.E. and van Steijn, H. (1990). Alpine debris flows and their sedimentary properties. A case study from the French Alps. *Permafrost and Periglacial Processes* **1**, 111-128.

Reichert, B.K., Bengtsson, L. and Oermans, J. (2002). Recent glacier retreat exceeds internal variability. *Journal of Climate* **15**, 3069-3081.

621 **Schär, C., Vidale, P.L., Lüthi, D., Frie, C., Häberli, C., Liniger, M. and Appenzeller, C. (2004).** The role of increasing temperature
622 variability in European summer heatwaves. *Nature* **427**, 332-336.

623 **Schlögel, R., Torgoev, I., De Marneffe, C. and Havenith, H.B. (2011).** Evidence of a changing distribution of landslides in the
624 Kyrgyz Tien Shan, Central Asia. *Earth Surface Processes and Landforms* **36(12)**, 1658-1669.

625 **Schmocker-Fackel, P. and Naef, F. (2010).** More frequent flooding? Changes in flood frequency in Switzerland since 1850.
626 *Journal of Hydrology* **381**, 1–8.

627 **Soldati, M., Corsini, A. and Pasuto, A. (2004).** Landslides and climatic change in the Italian Dolomites since the Late glacial.
628 *Catena* **55**, 141-161.

629 **Sorriso-Valvo, M. (2002).** Landslides: from inventory to risk. In: Landslides. Rybář, Stemberk and Wagner (Eds.). Swets &
630 Zeitlinger (Pubs.), Lisse, 2002.

631 **Squarzoni, C., Delacourt, C. and Allemand, P. (2005).** Differential single-frequency GPS monitoring of the La Valette landslide
632 (French Alps). *Engineering Geology* **79**, 215–229.

633 **Stark, C.P. and Hovius, N. (2001).** The Characterization of Landslide Size Distributions. *Geophysical Research Letters* **28(6)**, 1091-
634 1094.

635 **Szabó, J. (2003).** The relationship between landslide activity and weather: examples from Hungary. *Natural Hazards and Earth*
636 *System Sciences* **3**, 43-52.

637 **Theurillat, J-P. and Guisan, A. (2004).** Potential impact of climate change on vegetation in the European Alps: A review.
638 *Climatic Change* **50(1-2)**, 77-109.

639 **Torgoev, A.D., Torgoev, I.A., Aleshin, Y.G., Havenith, H.-B. and Schögel, R. (2010).** Assessment of landslide activity in the Maily-
640 Say Valley, Kyrgyz Tien Shan. In Mountain Risks: Bringing Science to Society, Mallet, Glade and Casagli (Eds.).

641 **Van Beek, L.P.H. and Van Asch, TH.W.J. (2004).** Regional assessment of the effects of land-use change on landslide hazard by
642 means of physically based modelling. *Natural Hazards* **31**, 289-304.

643 **Van Den Eeckhaut, M., Hervas, J., Jaedicke, C., Malet, J.-P. and Picarelli, L. (2010).** Calibration of logistic regression coefficients
644 from limited landslide inventory data for European-wide landslide susceptibility modelling. In Mountain Risks: Bringing Science
645 to Society, Mallet, Glade and Casagli (Eds.).

646 **Van Den Eeckhaut, M. and Hervas, J. (2012).** Landslide inventories in Europe and police recommendations for their
647 interoperability and harmonisation, *JRC Scientific and Policy Reports: A JRC contribution to the EU-FP& Safeland* Project., 2012.

648 **Varnes, D.J. (1978).** Slope movement types and processes. In: Schuster, R.L., Krizek, R.J. (Eds.), Special Report 176 Landslides:
649 Analysis and Control. Transportation Research Board, National Research Council, Washington D.C., pp. 11 – 33.

650 **WGMS (2013).** Preliminary glacier mass balance data 2010/2011, online from
651 http://www.geo.uzh.ch/microsite/wgms/mbb/sum11.html (Last accessed 19/12/2013).

Figure

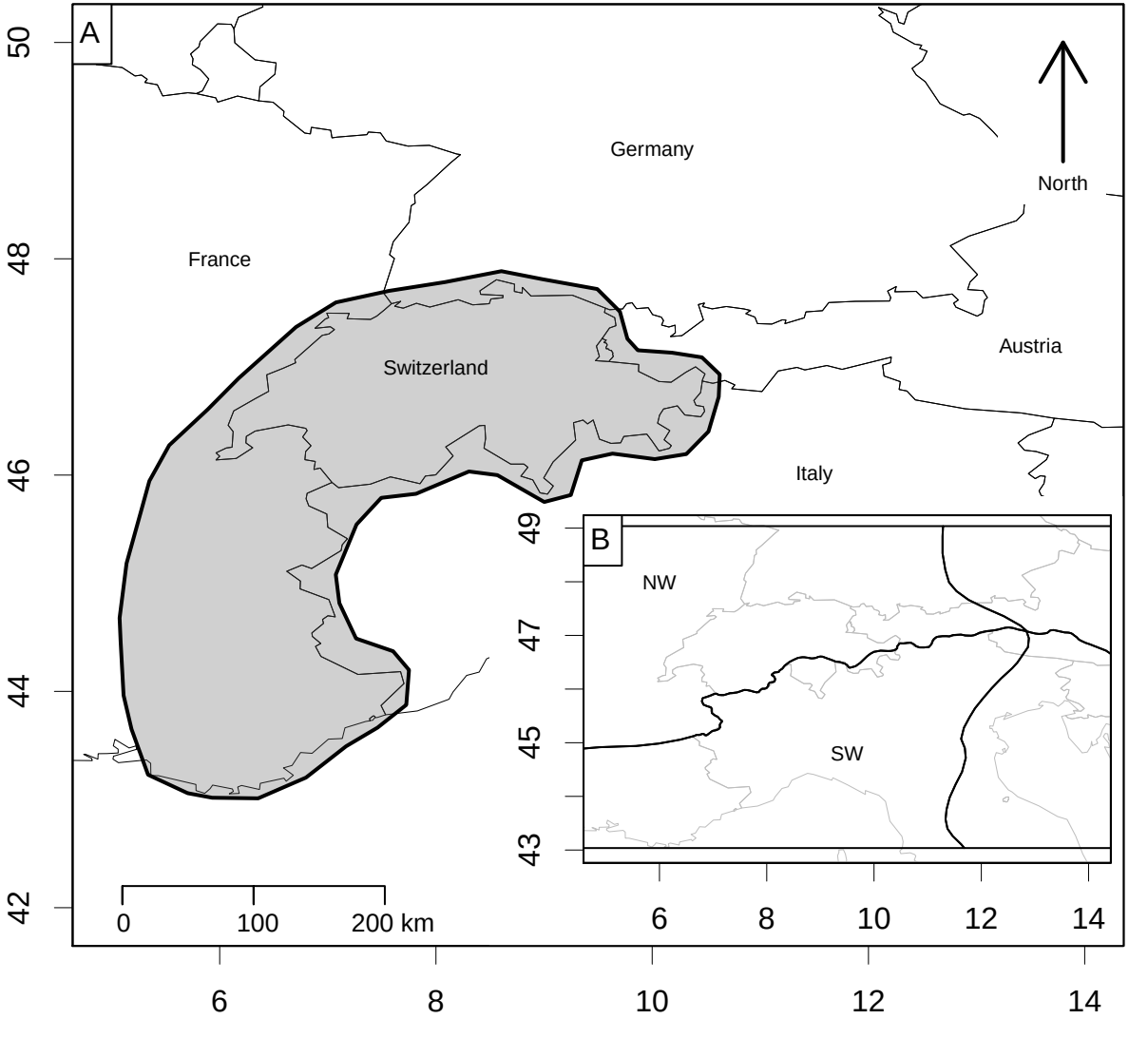
A
Germany
France
Switzerland
Austria
Italy
North
B
NW
SW
0
100
200 km
42
44
46
48
50
6
8
10
12
14
43
45
47
49

Figure

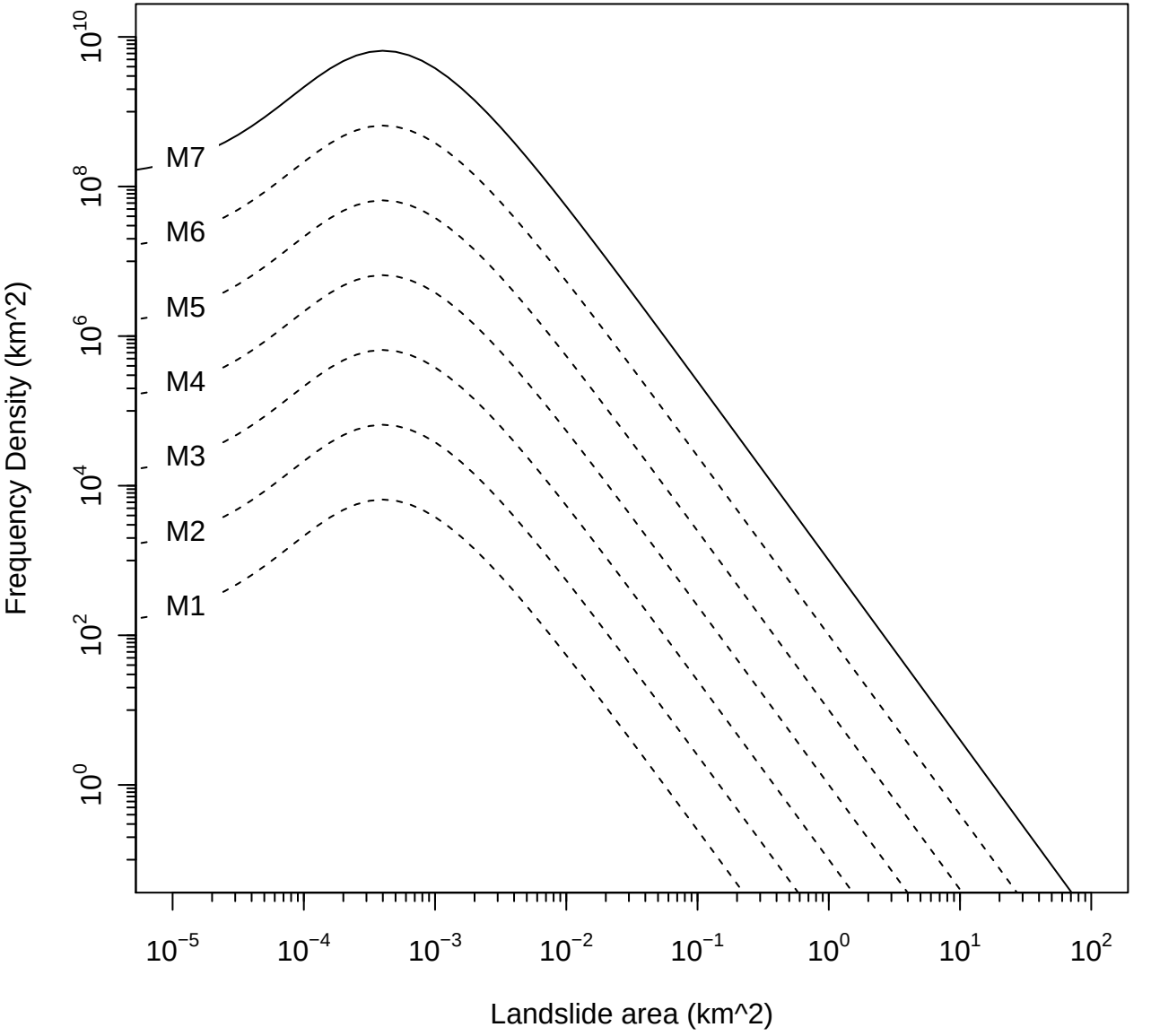
Frequency Density (km^2)
10^{0}
10^{2}
10^{4}
10^{6}
10^{8}
10^{10}
M7
M6
M5
M4
M3
M2
M1
10^{-5}
10^{-4}
10^{-3}
10^{-2}
10^{-1}
10^{0}
10^{1}
10^{2}
Landslide area (km^2)

Figure

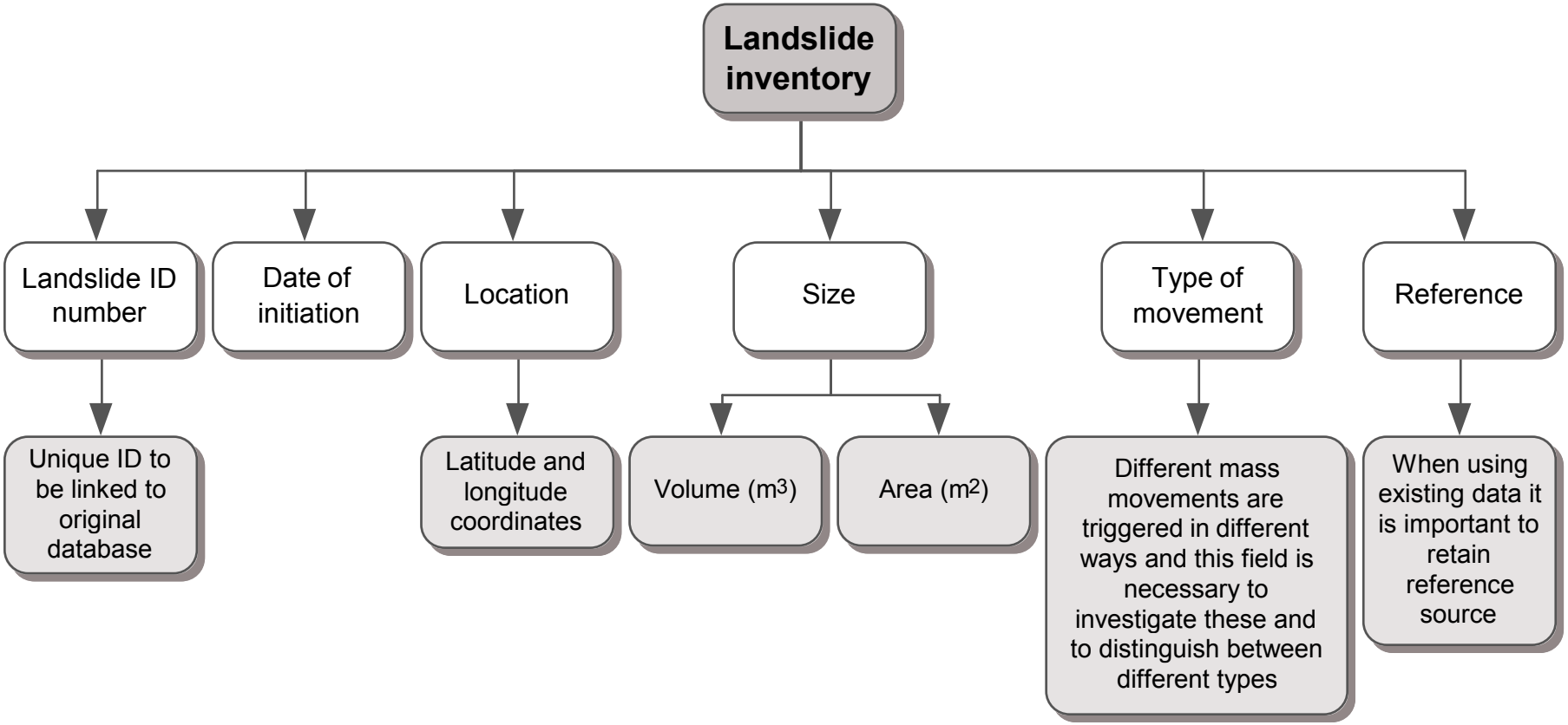
Landslide inventory
Landslide ID number
Date of initiation
Location
Size
Type of movement
Reference
Unique ID to be linked to original database
Latitude and longitude coordinates
Volume (m3)
Area (m2)
Different mass movements are triggered in different ways and this field is necessary to investigate these and to distinguish between different types
When using existing data it is important to retain reference source

Figure

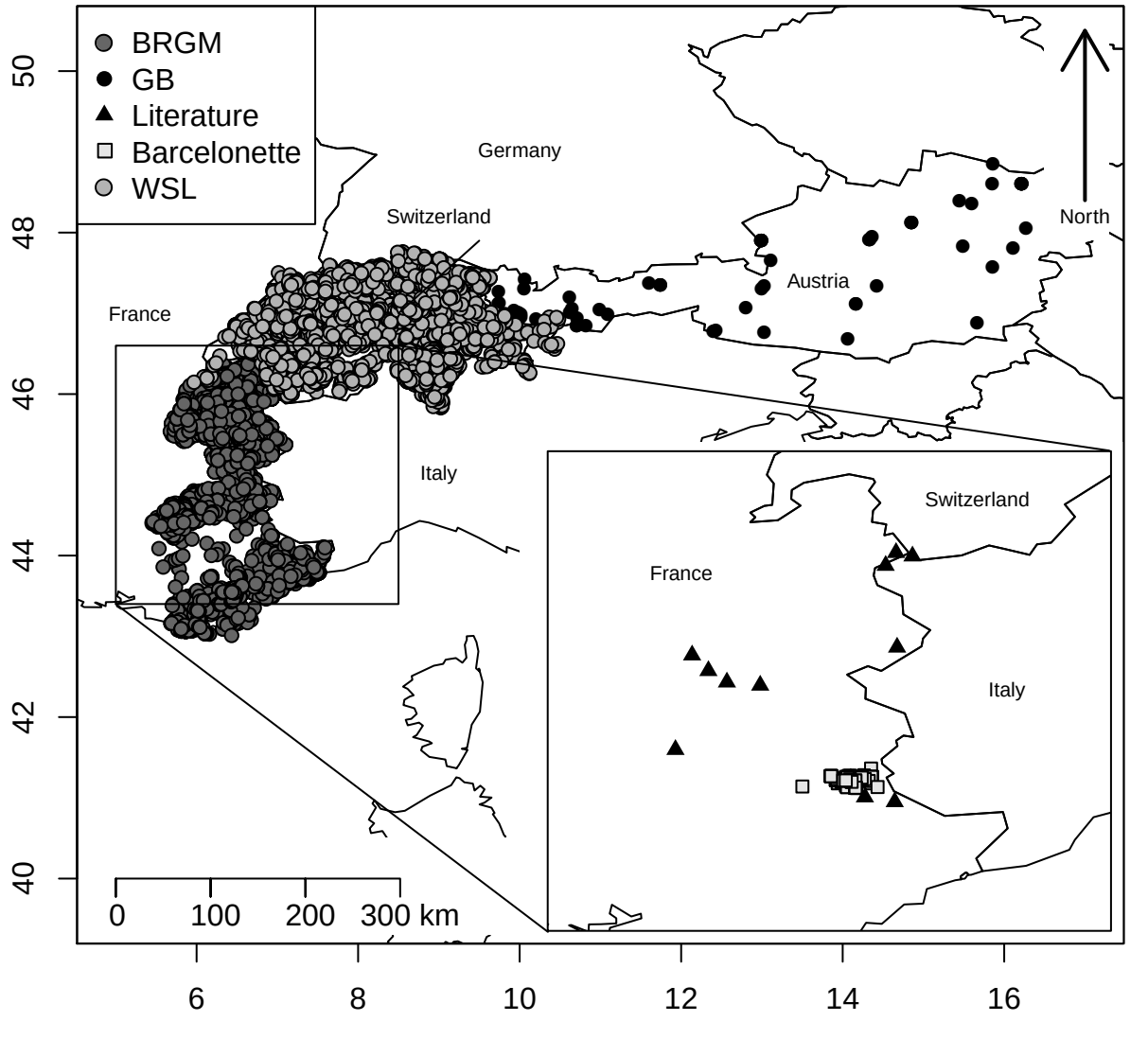
BRGM
GB
Literature
Barcelonette
WSL
Germany
Switzerland
Austria
France
Italy
North
0
100
200
300 km
40
42
44
46
48
50
6
8
10
12
14
16

Figure

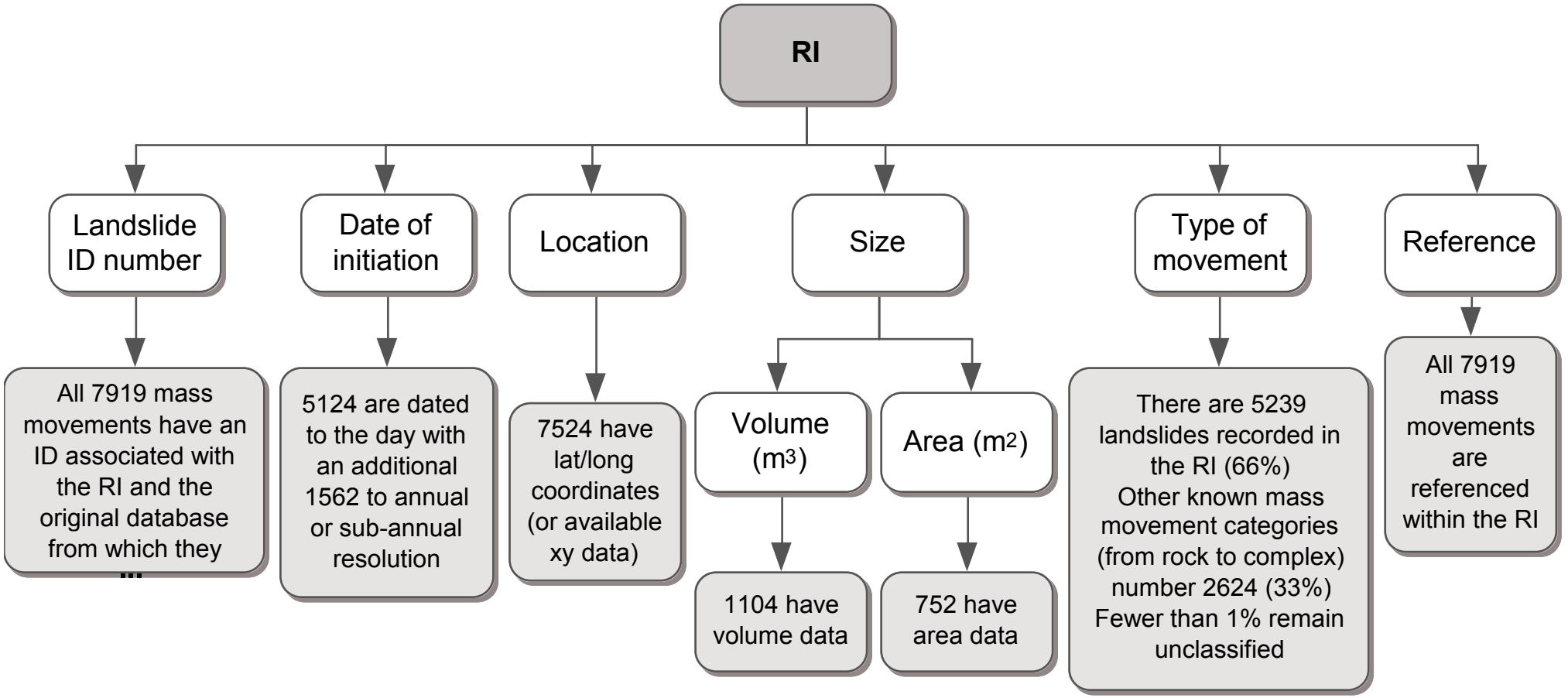
RI
Landslide ID number
Date of initiation
Location
Size
Type of movement
Reference
All 7919 mass movements have an ID associated with the RI and the original database from which they
5124 are dated to the day with an additional 1562 to annual or sub-annual resolution
7524 have lat/long coordinates (or available xy data)
Volume (m^3)
Area (m^2)
1104 have volume data
752 have area data
There are 5239 landslides recorded in the RI (66%)
Other known mass movement categories (from rock to complex) number 2624 (33%)
Fewer than 1% remain unclassified
All 7919 mass movements are referenced within the RI

Figure

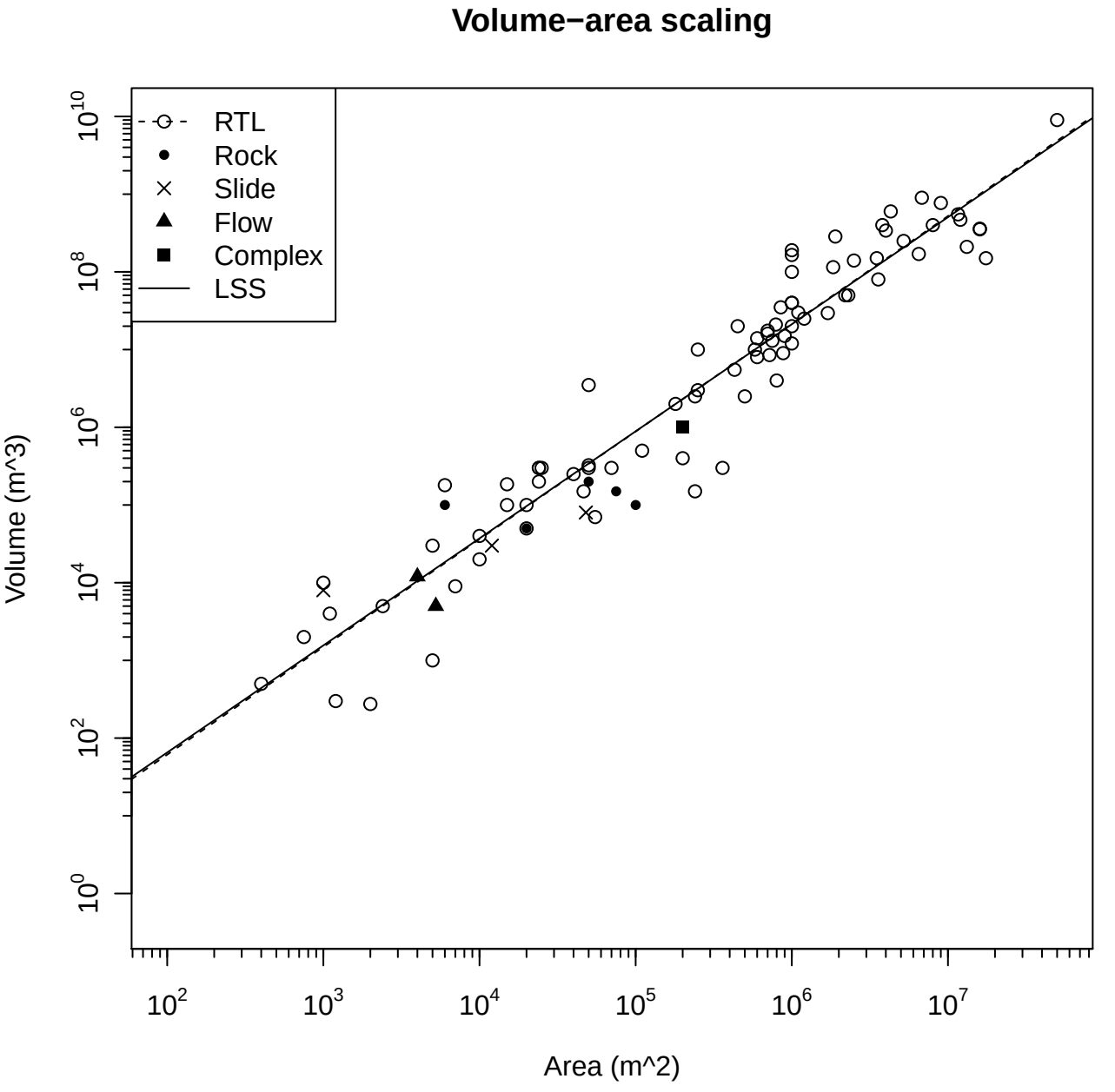
Volume−area scaling
RTL
Rock
Slide
Flow
Complex
LSS
Volume (m^3)
Area (m^2)
10^0
10^2
10^4
10^6
10^8
10^{10}
10^2
10^3
10^4
10^5
10^6
10^7

Figure

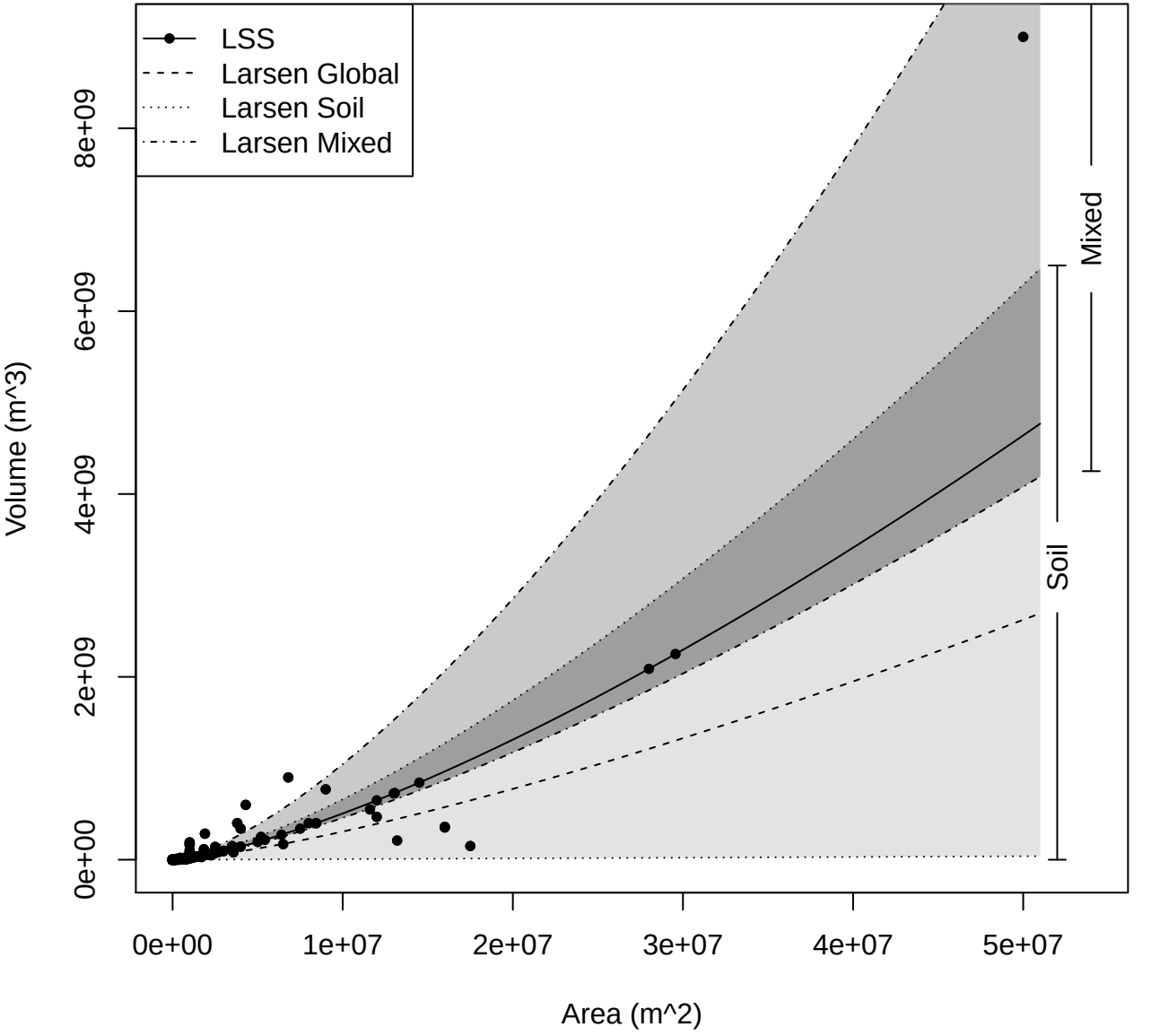
LSS
Larsen Global
Larsen Soil
Larsen Mixed
Volume (m^3)
0e+00
2e+09
4e+09
6e+09
8e+09
0e+00
1e+07
2e+07
3e+07
4e+07
5e+07
Area (m^2)
Soil
Mixed

Figure

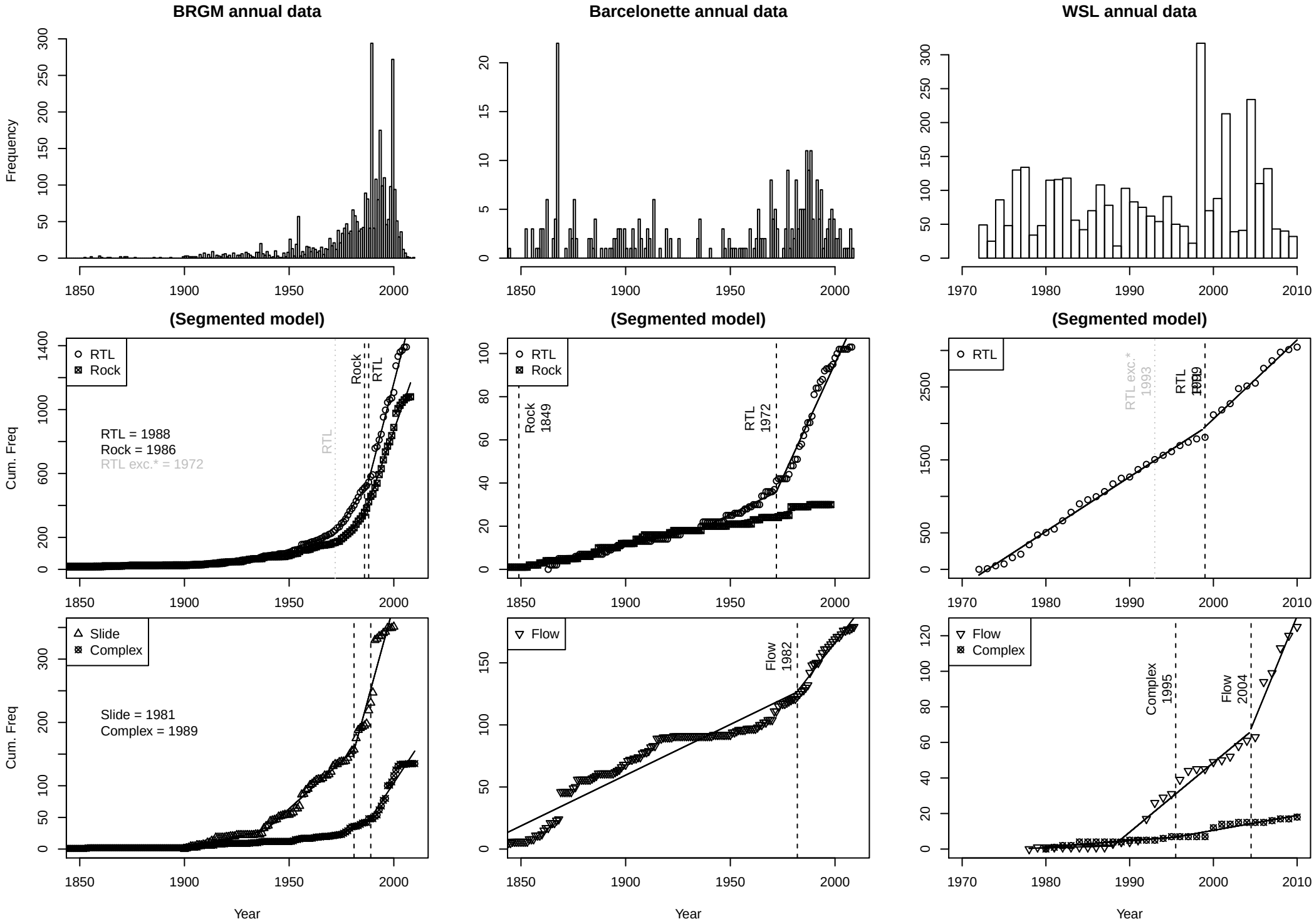
BRGM annual data
Barcelonette annual data
WSL annual data
Frequency
(Segmented model)
Cum. Freq
RTL
Rock
RTL = 1988
Rock = 1986
RTL exc.* = 1972
Rock 1849
RTL 1972
RTL exc.* 1993
RTL 1999
Slide
Complex
Slide = 1981
Complex = 1989
Flow
Flow 1982
Complex 1995
Flow 2004
Year

Figure

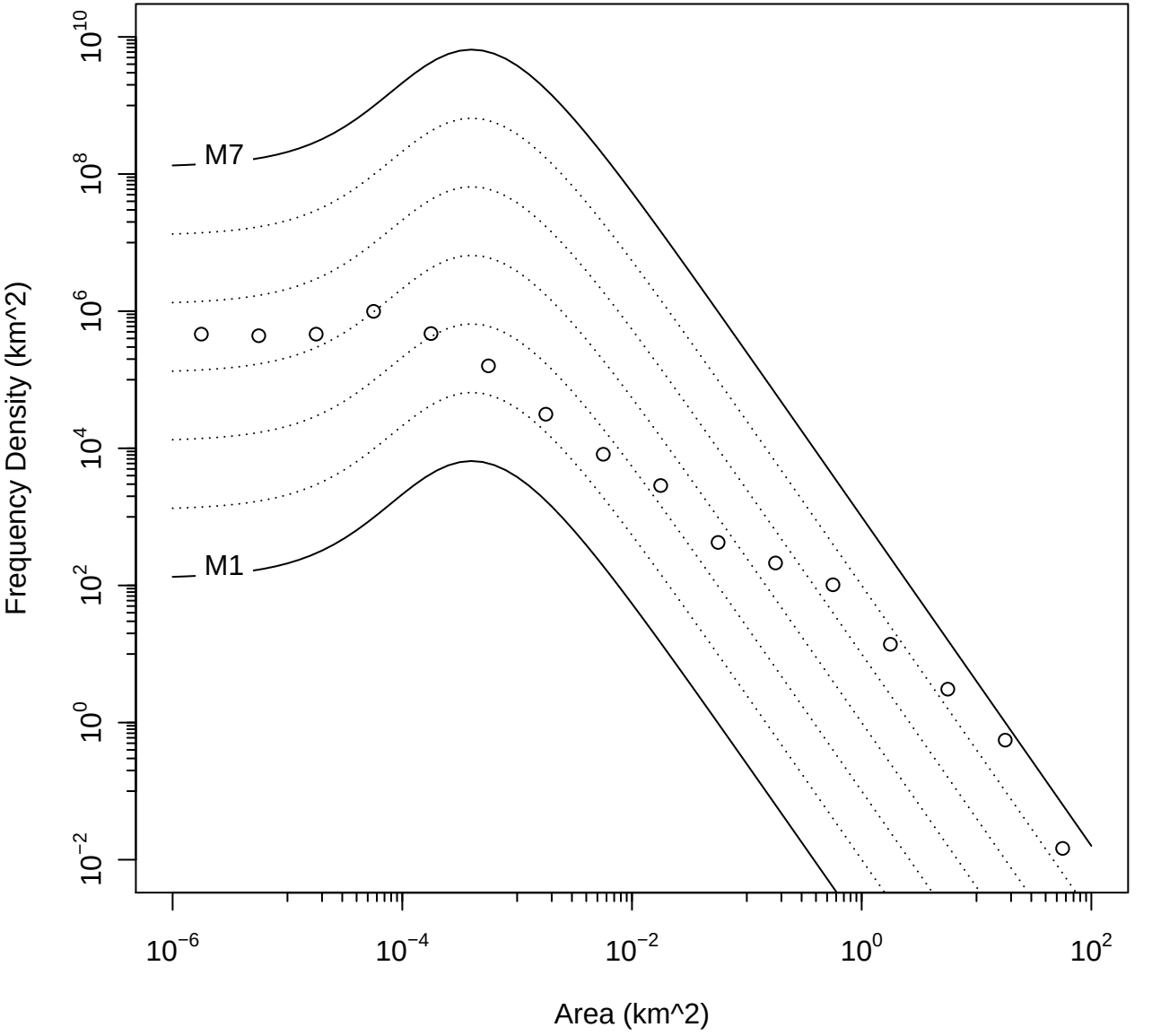
M7
M1
Frequency Density (km^2)
Area (km^2)
10^{-2}
10^{0}
10^{2}
10^{4}
10^{6}
10^{8}
10^{10}
10^{-6}
10^{-4}
10^{-2}
10^{0}
10^{2}

Figure

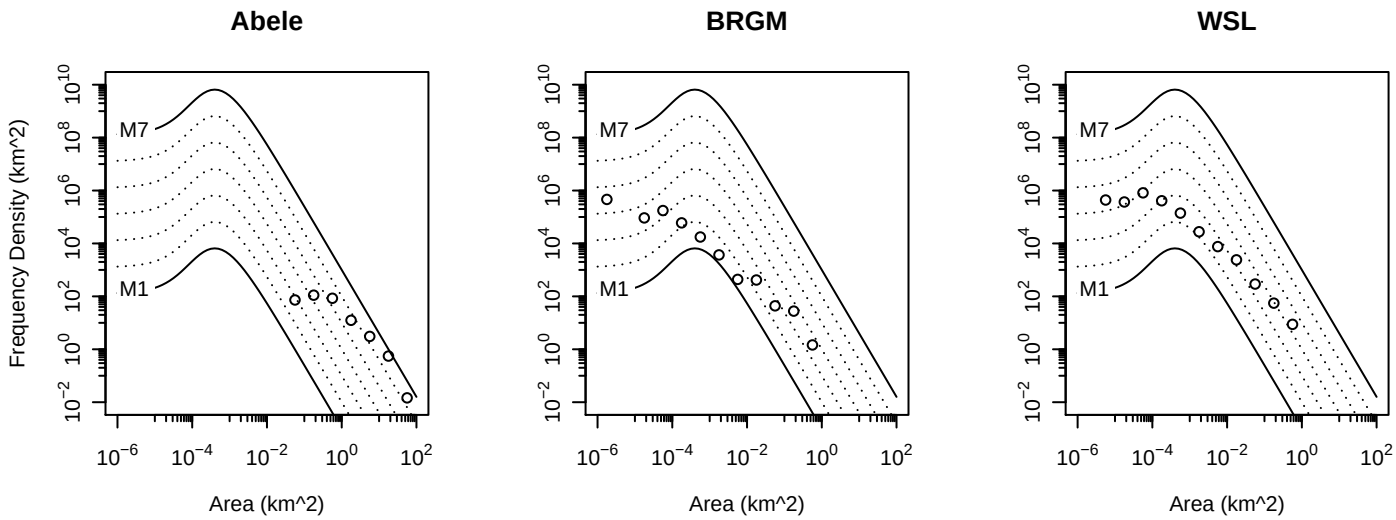

Figure

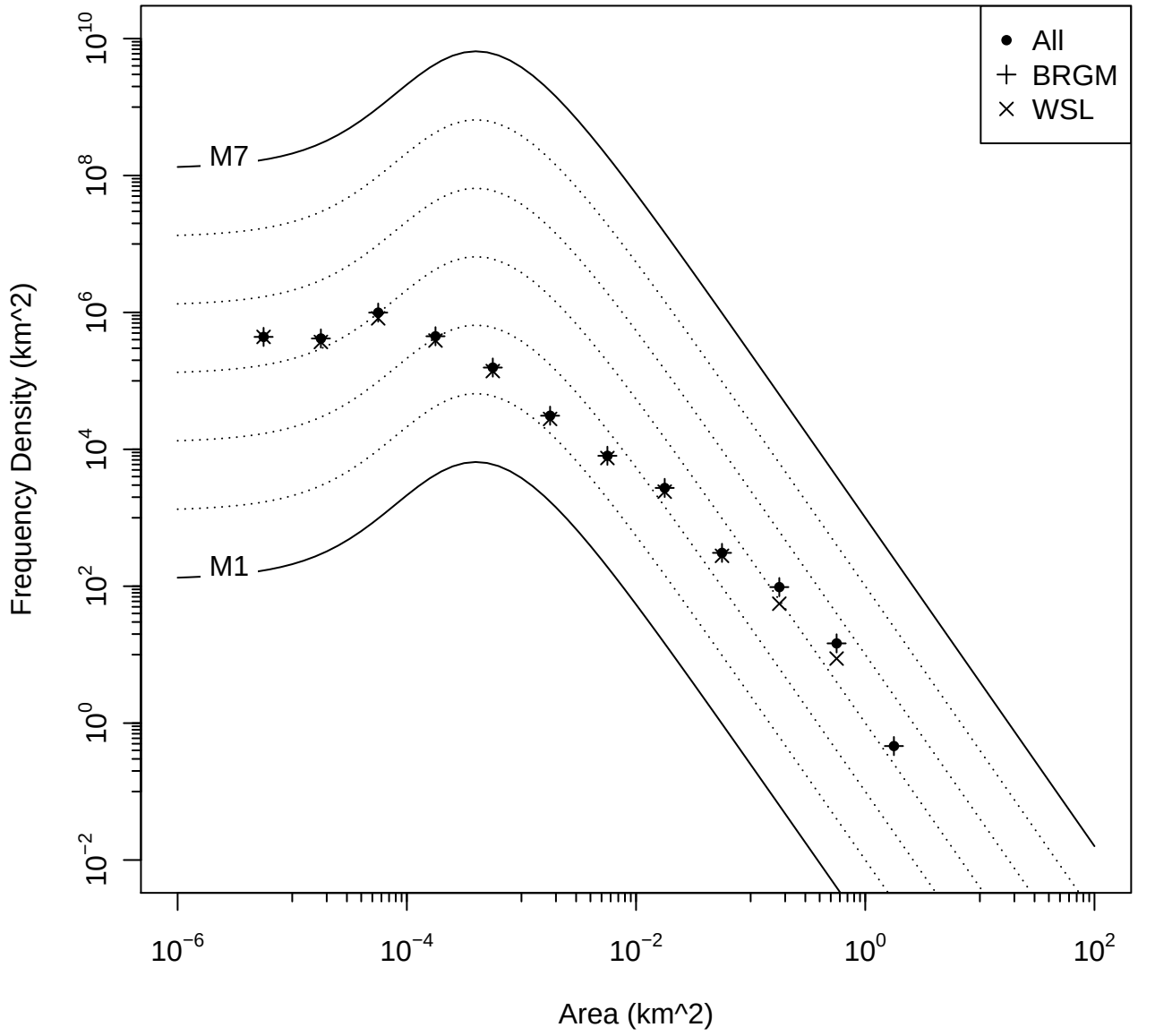
All
BRGM
WSL
M7
M1
Frequency Density (km^2)
Area (km^2)
10^{10}
10^{8}
10^{6}
10^{4}
10^{2}
10^{0}
10^{-2}
10^{-6}
10^{-4}
10^{-2}
10^{0}
10^{2}